8-27-2009

Novel method for carbon nanofilament growth on carbon fibers

Daniel Garcia

Daniel Garcia
Candidate

Mechanical Engineering
Department

This thesis is approved, and it is acceptable in quality and form for publication on microfilm:

Approved by the Thesis Committee:

Dr. Marwan Al-Haik, Chairperson

Dr. Claudia Luhrs 05/14/09

Dr. Jonathan Phillips

NOVEL METHOD FOR CARBON NANOFILAMENT GROWTH ON CARBON FIBERS

BY

DANIEL GARCIA

PREVIOUS DEGREES
BACHELORS IN SCIENCE MECHANICAL ENGINEERING
UNIVERSITY OF NEW MEXICO
FALL 2007

THESIS

Submitted in Partial Fulfillment of the
Requirements for the Degree of

Master of Science in Mechanical Engineering

The University of New Mexico
Albuquerque, New Mexico
August 2009

DEDICATIONS

This thesis is dedicated to my family for always supporting me during my academic career. Particularly I would like to dedicate this work to my mother who has instilled in me the importance of an education.

ACKNOWLEDGEMENTS

A great deal of thanks is due to the numerous people who aided me in preparing this document in one way or another. My advisor Dr. Al-Haik is owed the biggest recognition for continually providing his insight along each step of the project and being patient in guiding me through its completion. I would also like to thank the members of the committee Dr. Phillips and Dr. Luhrs who each provided me with plenty of feedback about my work and each spent a significant amount of time both helping me run experiments and understand the theory of the work. Finally, special recognition goes to my fellow students on the research team who helped me finish the work presented in this thesis: Jeremy Chavez, Juanita Trevino, Mark Atwater, and Mehran Tehrani.

NOVEL METHOD FOR CARBON NANOFILAMENT GROWTH ON CARBON FIBERS

BY

DANIEL GARCIA

ABSTRACT OF THESIS

Submitted in Partial Fulfillment of the
Requirements for the Degree of

Master of Science in Mechanical Engineering

The University of New Mexico
Albuquerque, New Mexico

August 2009

Novel Method for CARBON NANOFILAMENT GROWTH on CARBON FIBERS

By:

Daniel Garcia

B.S., Mechanical Engineering, University of New Mexico, 2007

M.S., Mechanical Engineering, University of New Mexico, 2009

ABSTRACT

Carbon nanofilaments were grown on the surface of microscale carbon-fibers at relatively low temperature using palladium as a catalyst to create multiscale fiber reinforcing structures with potential applications in structural composites. Employing a relatively new method, in which carbon structures are grown from fuel rich combustion mixtures on certain catalytic metals, multiscale filament structures were grown from ethylene/oxygen mixtures at 550 °C on commercial PAN and pitch carbon fibers. The filaments grew in a bimodal size distribution. Relative short, densely spaced nanofilaments (ca. 10 nm diameter), and a slightly less dense layer of larger (ca. 100 nm diameter) faster growing fibers (ca. 10 microns/hr) were found to exist together to create a unique multiscale structure. All analytical techniques employed indicated poor crystallinity of the produced filaments.

Table of Contents

LIST OF FIGURES viii

CHAPTER 1: INTRODUCTION

1.1 ROLE OF CARBON NANOFIBERS/NANOTUBES……1
1.2 CARBON NANOSTRUCTUERS 2
1.3 THEORY OF GROWTH OF CARBON FILAMENTS……..11
1.4 THESIS OUTLINE……..……15

CHAPTER 2: CARBON FILAMENT GROWTH: STATE OF THE ART

2.1 METHODS OF SYNTHESIS FOR CARBON NANOFILAMENTS ON CARBON FIBERS…… 17
2.2 GRAPHITIC STRUCTURES BY DESIGN (GSD)……..22

CHAPTER 3: USE OF PALLADIUM AS A CATALYST FOR GROWTH

3.1 EXPERIMENTAL: STANDARD PROTOCOL……26
3.2 SUBSTRATES FOR GROWTH……30
3.3 REMOVAL OF THE SIZING……32
3.4 ACTIVATION BY BURNING PRETREATMENT……...33
3.5 IMPREGNATION OF CATALYST VIA INCIPIENT WETTING……33
3.6 GROWTH STEP: FILAMENT GENERATION……35
3.7 VARIATIONS OF SIZING REMOVAL……36
3.8 INITIAL TRIALS OF INCIPIENT WETTING AND PROOF OF CONCEPT ……41
3.9 EFFECT OF CHANGING THE CARBON FIBER SUBSTRATE……...53
3.10 TRANSMISSION ELECTRON MICROSCOPY (TEM) CHARACTERIZATION……56
3.11 X-RAY DIFFRACTION CHARACTERIZATION……59
3.12 TEMPERATURE PROGRAMMED OXIDATION…….. ……62

CHAPTER 4: CONCLUSIONS AND FUTURE WORK

4.1 BASIC OBSERVATIONS ABOUT GSD PROTOCOL……65
4.2 EFFECT OF PARAMETERS ON FILAMENT SIZE……..66
4.3 EFFECT OF POSITION OF CHAMBER ON CNF GROWTH……...67
4.4 EFFECT OF SUBSTRATE ON CNF GROWTH……....67
4.5 EFFECT OF TEMPERATURE ON CNF GROWTH……...68
4.6 EFFECT OF 'ENHANCED PARAMETERS' ON CNF GROWTH……...68
4.7 FUTURE WORK OF CNF GROWTH PROTOCOL……...69
4.8 FUTURE APPLICATION OF RESEARCH……....70

REFERENCES……73

List of Figures

FIGURE 1.2-1 Different Structures of Carbon.....4
FIGURE 1.2-2 (a) C_{60} buckeyball (b) C_{70} buckeyball [12]……..6
FIGURE 1.2-3 Atomic structure of a single-wall carbon nanotube [12]……..8
FIGURE 1.2-4 Illustration of 3 cases of interaction between a liquid deposit (A) and a substrate B: island growth for non-wetting case (I) and wetting case (II) and layer growth for (III) with corresponding conditions of surface energies of the substrate [18]…….11
FIGURE 1.3-1 Two common types of carbon filament growth [18]…….13
FIGURE 1.3-2 (a) Electron microscope image of CNF growing in two directions off a catalytic particle. (b) zoomed in image of (a) showing the atomic planes. (c) diagram depicting the atomic planar arrangement shown in parts (a) and (b). (d) electron microscope image of a multi-walled carbon nanotube. [19]…….14
FIGURE 2.2-1 Different Morphologies resulting from varying environment of Nickel nanoparticles [32]……...23
FIGURE 2.2-2 Illustration of importance of placement of sample during deposition in the GSD process (a) shows graphite lattice placed 7 cm upstream form the heating element while (b) shows a graphite lattice samples that was directly underneath the heating element during the GSD process [32]……...….24
FIGURE 3.1-1 Schematic of chamber used in Lindberg Hevi-Duty® furnace……..27
FIGURE 3.1-2 Temperature profile of Lindberg Hevi-Duty® furnace [33]……..28
FIGURE 3.1-3 Schematic of ‘long’ chamber used in Lindberg Blue M furnace; the ‘short’ chamber utilized only zone 1 for heating……...29
FIGURE 3.1-4 Temperature profile of Lindberg Blue M furnace……..30
FIGURE 3.2-1 Scanning Electron Micrograph of short chopped PAN carbon fiber as received from manufacturer……...31
FIGURE 3.7-1 Results of heat treatment only (500° C in O_2) in removing the sizing…...37
FIGURE 3.7-2 Micrograph of sample for corresponding locations (A, B, and C) analyzed under EDS (spot analysis) whose spectrums are shown in Figure 3.7-3……...38
FIGURE 3.7-3 EDS analysis of sample after heat treatment (A, B, and C represent the spectrums of each respective location)……..39

FIGURE 3.7-4 Results of heat treatment and rinsing in removing the sizing……40
FIGURE 3.7-5 Temperature Profile used to burn sizing in air……...41
FIGURE 3.8-1 Sample after initial trials of incipient wetting (a) 185 % Pd loading (b) 326 % Pd loading (c) 467% Pd loading……43
FIGURE 3.8-2 Sample after incipient wetting (19.4 % Pd loading) showing 2 morphologies of Pd deposited……45
FIGURE 3.8-3 Two setups used for the incipient wetting technique (a) employs no sonication while (b) uses sonication……..46
FIGURE 3.8-4 Samples after one minute deposition using the (a) sonicated incipient wetting protocol and the (b) non-sonication incipient wetting protocol……48
FIGURE 3.8-5 Sonicated sample after 5 minute deposition showing 2 modes of growth.50
FIGURE 3.8-6 Sample after incipient wetting with sonication showing an agglomeration of Pd particles via (a) scanning electron micrograph and (b) backscattered electron micrograph. (c) shows islands growth of Pd particles……...51
FIGURE 3.9-1 Pitched based fiber with deposition time of 35 minutes showing uniform coating of nm scale filaments……54
FIGURE 3.9-2 Micrographs of long PAN based fibers after 35 minute deposition……..55
FIGURE 3.10-1 Transmission Electron Micrograph showing 2 layers of filament growth and proof of tip-based growth (scale of 100 nm)……...57
FIGURE 3.10-2 Transmission Electron Micrograph showing parent fiber (dark upper left corner) and nanofilaments (lighter bundle coming off of parent fiber). (scale of 50 nm).58
FIGURE 3.10-3 Transmission Electron Micrograph showing amorphous character and tip based growth……59
FIGURE 3.11-1 Schematic of X-Rays being diffracted by a crystal illustrating physical meaning of variables in Bragg's law [39]…….60
FIGURE 3.11-2: XRD diffractogram of Carbon Fibers with CNF from 90 minute growth protocol 0.5% loading of Pd…….61
Figure 3.11-3 XRD diffractogram of Bare PAN short chopped carbon fibers……62

Figure 3.12-1 Comparison of different levels of graphitization of carbon including carbon fibers with filaments……..64
Figure 4.10-1 Fiber Pullout: fracture surface from tensile test [47]…….71

CHAPTER 1: INTRODUCTION

1.1 Role of Carbon Nanofibers/Nanotubes

Carbon nanotubes (CNTs) have sparked great interest in the engineering community ever since they were first discovered in 1991 by Dr. Sumio Iijima through an arc discharge process [1]. Carbon nanotubes are specific family of carbon nanofiber (also referred to as a carbon filament) that consist of crystalline graphitic sheets that are rolled up into a hollow, cylindrical shape [2]. The arc discharge process itself involves temperatures as high as 3000°C where carbon atoms are evaporated with high enough energy to grow CNTs with an inner diameter (ID) as small as 0.7 nm. Several other synthesis processes, at much lower temperatures, have been utilized to grow CNTs. Interest in CNTs has grown extensively since their discovery because they possess many potentially useful properties such as very high thermal conductivity, and extremely high tensile strength and Young's modulus. Some applications that have already been demonstrated include electromechanical actuators, random access memory (RAM) devices, field effect transistors and atomic force microscope (AFM) probes [3]. There are also many novel areas where CNTs are being investigated for possible use such as the use of CNTs as space elevators where due to their superior stiffness to weight ratio [4].

While CNTs might be considered relatively new, it should be noted that with the aid of electron microscopy carbon products in tubular form have been observed since the 1950s [5]. One of the first records of growth of filamentous carbon goes back even further to a U.S. patent from 1889 [6] which demonstrated that catalytic decomposition of a carbon

containing gas on a hot metal surface (in this case an iron crucible) causes carbon nanofiber to form. In the next century many papers have been published on carbon nanofiber and carbon nanotubes synthesis and applications (some of which will be mentioned in section 2.1). A final note: in the course of research publications it is common to see variations in the nomenclature of carbon nanotubes and carbon nanofibers whether it be describing carbon filaments as carbon whiskers, filaments, or even as carbon nanotubes even if the structures are not by conventional definition considered nanotubes. For this thesis carbon nanofibers will be appreviated as CNFs or called filaments as no appreciable amount of carbon structures in the current work are by conventional definition carbon nanotubes.

1.2 Carbon Nanostructures

While CNTs have sparked the greatest recent interest of any form of carbon structures, it is important to note that other forms of carbon also display properties and physical characteristics comparable to those of carbon nanotubes. An example is graphene, a plane of sp^2 bonded carbon atoms packed in a honeycomb crystal lattice, which via an atomic force microscope tip its Young's modulus was measured to be 0.5 TPa which is of the same order as the Young's modulus from various types of CNTs [7]. Therefore the value of carbon nanostructures as a potential solution to many modern engineering problems should not be limited to only CNTs.

The properties in carbon structures all relate to the orientation of the carbon atoms in the various forms of carbon. In general, carbon atoms have six electrons which can occupy

$1s^2$, $2s^2$, and $2p^2$ atomic orbitals. The difference of properties between the different forms of carbon can be attributed to the different hybridizations carbon atoms can take: sp, sp^2, and sp^3 which correspond to chain, planar and tetrahedral structures respectively. Carbon atoms form extremely strong covalent bonds but based on which hybridization it take, the bonds out of a plane of carbon atoms may be much weaker Van Der Wall bonds (such as for graphite which is stacked planes of graphene). An example of the effect of the carbon structure on its properties is that electrical transport properties are far superior in plane of a graphene plane than in between graphene planes. There are many more such as hardness, chemical reactivity, and magnetic and optical properties. Figure 1.2-1 shows various carbon structures which have different types of hybridizations: sp^3 for (a) while (b)-(e) are all have sp^2 bonding. The fact that CNFs and CNTs both have the same bonding (albeit different properties) indicates knowledge about one type of carbon structures greatly lends itself to knowledge about another.

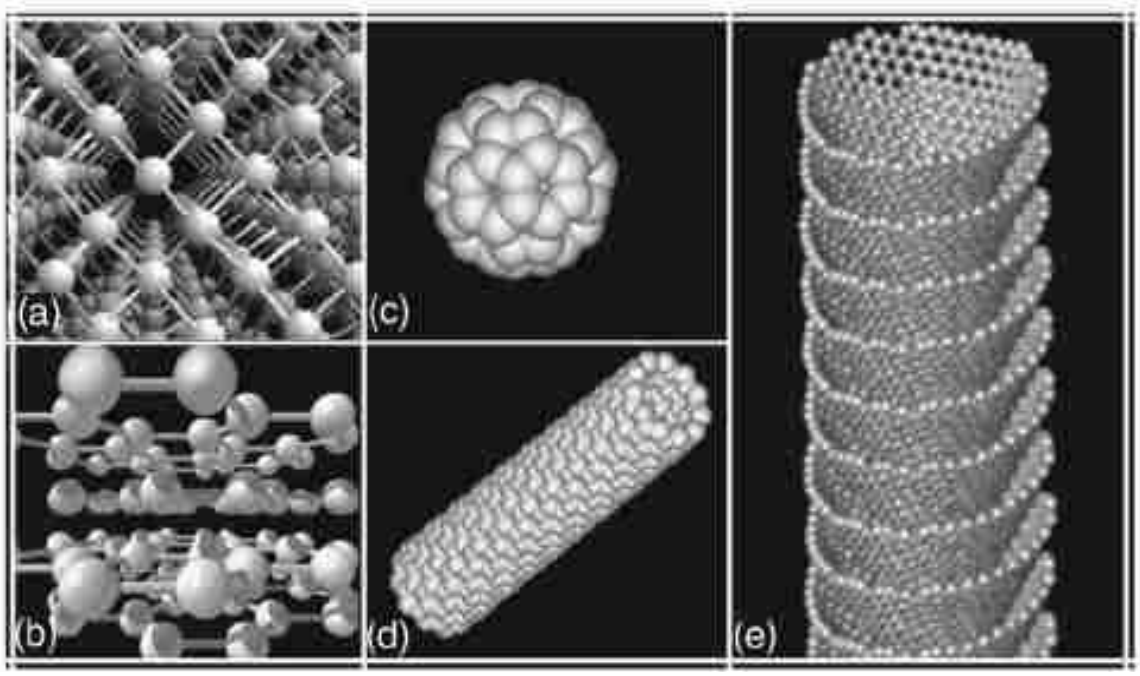

Figure 1.2-1: Different Carbon structures: (a) diamond (b) graphite (c) buckminster fullerene (d) single walled carbon nanotubes and (e) stacked cone carbon nanofiber [8]

There are numerous types of carbon fibers. CNFs are carbon fibers 3-100 nm in diameter and 0.1-1000 μm in length [9]. CNFs are composed of modified graphene sheets which may be stacked in different orientations. Generally, CNFs may be classified as herring (or fishbone) if the stacked graphite layers form cones or bamboo type if they form cups (nomenclature is based on the appearance of CNFs under transmission electron microscopy) [8]. CNTs are an example of parallel type CNFs, where the graphene sheets are continuous and parallel to the axis of the fiber (resulting in enhanced properties). They have been found to be either single walled (having one layer of graphene) where they are called SWCNTs or multi walled (having multiple layers of graphene) where they are abbreviated as MWCNTs. Another type of carbon fiber is the fishbone type where the

atomic planes are stacked at an angle to the axis of the fiber [10]. MWCNTs were the first CNTs to be discovered in the 90's though an arc-discharge process. Within a few years the technology had progressed to grow single-SWCNTs [1]. Eventually it was shown that *catalytic carbon nanofiber growth* (CCNF) mechanism could lead to the formation of SWCNTs (with tube diameters of 1-5 nm) albeit at high temperatures (>1000°C) [11]. Although the physical molecular growth mechanisms of these nanotubes can be quite complex, it is possible to get a basic understanding of how CNTs grow by examining the simpler, single-walled case. One of the most thorough growth mechanisms for SWCNTs has been proposed by W. Deng et al. [12].

It has been observed that carbon nanotubes have a structure that is fullerene in nature; the simplest CNT can be represented by a buckminsterfullerene molecule- also known as a "buckeyball" as shown in Figure 1.2-2. The geometry of buckminsterfullerene is an Archimedean Solid called a truncated icosahedron, which looks like a soccer ball. The simplest buckeyball consists of 60 carbon atoms arranged into 12 pentagonal faces and 20 hexagonal faces; if the buckeyball is regular it will have a vertex configuration of (5, 6,6) and the pentagonal faces will be evenly spaced. Using Euler's formula as shown in equation (1.1), it can be proven that exactly 12 pentagonal faces are necessary to create the 360 degrees of curvature required for the buckeyball to be spherical, and a buckeyball can have as many hexagonal faces as it wants. Twelve Pentagons is always the minimum number required to fully "close" a fullerene structure, and the structure will always be spherical if the pentagonal faces are evenly and symmetrically spaced [12].

$$V + E + F = 2 \qquad (1.1)$$

where V is the number of vertices in any polyhedron, E is the number of edges in any polyhedron, and F is the number of faces in any polyhedron.

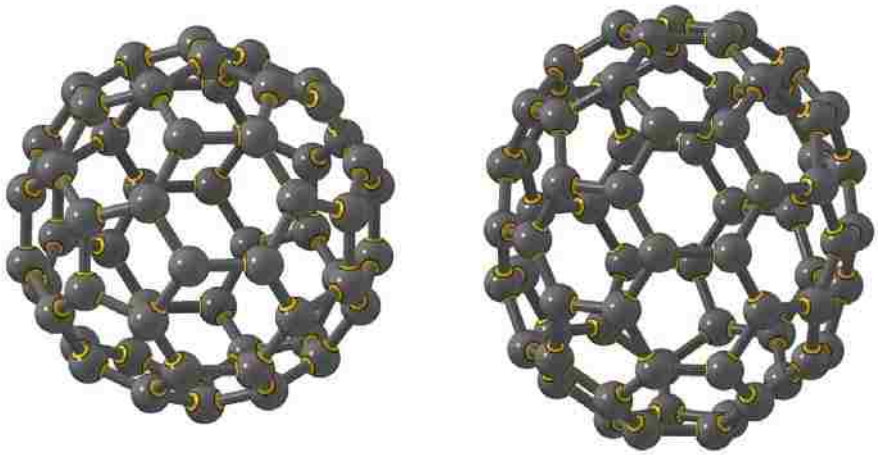

(a) (b)

Figure 1.2-2: (a) C_{60} buckeyball (b) C_{70} buckeyball [12]

Buckeyballs can also be made up of 70 carbon atoms instead of 60; in this case there will still be 12 pentagonal faces, but the number of hexagonal faces will increase. The buckeyball is no longer a regular polyhedral, it has started to elongate. It can be seen that if the buckeyball was to continue to elongate in this fashion it would become a CNT. Using Euler's formula again, we can see that when hexagonal faces are combined into a crystal lattice they will form into a flat plane. When this plane is rolled up, it will form a carbon nanotube. Thus an idealized CNT can be described as a seamless hexagonal lattice tube with 5,5,6,6 defects at the tip that close the tube and end its growth.

The theory proposed by W. Deng et al. [12] proposes that when atoms of carbon start to combine into fullerene structures, they can follow one of two paths in growth. If left alone, the carbon atoms will combine into buckminsterfullerene molecules like those shown in Figure 1.2-2 because this is the lowest energy fullerene configuration. However, if there is a catalyst present, the buckyball will only grow halfway around, and then the metal particles will provide a circular surface for the atoms on the incomplete edges of the buckeyball to bind to. The metal will catalyze the reaction so that only hexagonal faces are produced. It does this by helping to "fix" the pentagonal faces (i.e. change them into hexagonal faces) that occur naturally because this atomic arrangement is 1.7 eV lower energy than the hexagonal arrangement. As seen in Figure 1.2-1(a), the natural arrangement of carbon in fullerenes is to have 2 pentagonal faces on the sides of 2 connected hexagonal faces. This is called a 5,5,6,6 defect because this kind of connection closes the ends of carbon nanotubes and stops their growth. W. Deng et al. [12] propose the metal catalytic particles anneal the 5,5,6,6 defects into a 6,6,6,6 plane. This arrangement is shown in the Figure 1.2-3.

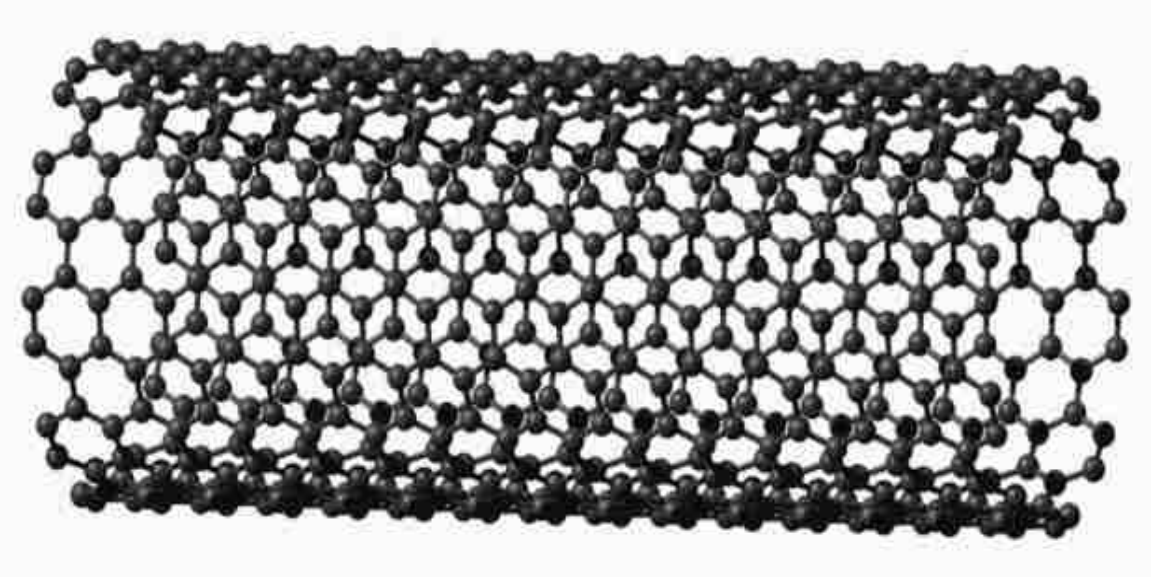

Figure 1.2-3 Atomic structure of a single-wall carbon nanotube [12]

The growth of multi-walled CNTs is presumed to be similar to the growth of single-walled CNTs, but there are many layers in the walls of the tubes instead of just one. The layers are stacked in a parallel type configuration and the thickness of the MWCNTs walls are determined by amount of time the fibers were allowed to grow; longer growth times lead to more layers and thicker sidewalls. Since CNTs are a specific type of CNF the growth models of CNTs may be applied in a general sense to those of CNFs.

Along with taking into account the actual growth mechanism of CNFs, it is important to note the role of the catalyst; the metal nanoparticles. While pure transition metals are often used such as iron, cobalt and nickel, alloys are sometimes used as well such as Cu-Ni. Molybdenum has also been used as a catalyst for growth using carbon monoxide as carbon feedstock [11]. Jong et al. [13] showed that varying the Cu

percentage in one-dimensional Cu-Ni impregnated structured carbon materials synthesized in a microwave enhanced vapor deposition system resulted in dramatically different morphologies in said materials. At 20% Cu via transmission electron microscopy (TEM) they observed that the carbon material produced were CNTs similar to those produced by using Ni as a catalyst. Further, they noticed that the morphology of the carbon material changed with the concentration of Cu: at 40% Cu the carbon produced was in filament form while at 80% Cu the carbon produced was in spiral form.

Along with the effect of varying the concentration of the alloy catalytic particles, it has been demonstrated that modifying the metal catalyst can be play in important role in CNF synthesis. Krishnankutty et al. [14] demonstrated a 2% copper to iron increase yielded 20 times the amount of CNFs in comparison to those produced with only pure iron at 600°C. The CNFs were synthesized in a Lindberg tube furnace where an ethylene/hydrogen mixture (1:4) was flowed for 5 hours. Different combinations of the Cu-Ni alloy were employed for comparison in the study. Doping the catalyst has also been shown to improve the synthesis process. Work by Tao et al.[15] in synthesizing multi branched CNTs has shown that doping Cu based catalysts with alkali elements spreads the catalyst better than the undoped catalysts improving their reactivity. It has also been observed that doping with an alkali metal (>0.1% w/w) increases the overall order of CNFs produced while also increasing the occurrences of helical structures in the filaments [16].

For the actual morphology of the metal nanoparticles (whether they comprise one metal or an alloy), understanding the wetting contact angle between catalytic solutions and the substrate is important in understanding the nucleation and growth mechanisms of the metal nanoparticles. If the surface of the substrate is hydrophobic (repels water), an aqueous solution of the metal salt will not adhere well and thus very little or no catalyst particles may be formed on the surface. Hydrophilic surfaces will in turn allow an aqueous solution containing a metal salt to settle and wet it to from catalytic nanoparticles for growth. To predict the shape that a catalytic nanoparticle may take upon annealing after a film is formed Young's equation as given in equation (1.2) must be considered

$$\gamma_s - \gamma_L = \cos\theta + \gamma_{SL} \tag{1.2}$$

where γ_s is the solid surface free energy, γ_L is the liquid surface free energy, θ is the contact angle between the liquid and substrate, and γ_{SL} is the solid/liquid interfacial free energy.

Figure 1.2-3 shows a physical description of 3 possible outcomes of physically depositing a metal on a substrate along with the conditions of the substrate surface energy that are needed for the outcome to occur. The condition that determines whether the growth is in the form of isolated islands of fibers or in the form of continuous films is if $\gamma_B + \gamma_{AB}$ is greater than γ_A. If this condition is fulfilled, then the Volmer-Weber effect will occur leading to the creation of islands of the catalytic particle [17] . If not, the film growth will occur instead. For growth of CNFs via catalytic metal nanoparticles, the desired contact angle lies around the middle of the possible spectrum of contact angles (0°-180°)

as a contact angle of 0° would represent a hydrophilic surface where an undesired metal film would be present and 180° would represent a hydrophobic surface where the nucleation would actually be homogenous which is not desired.

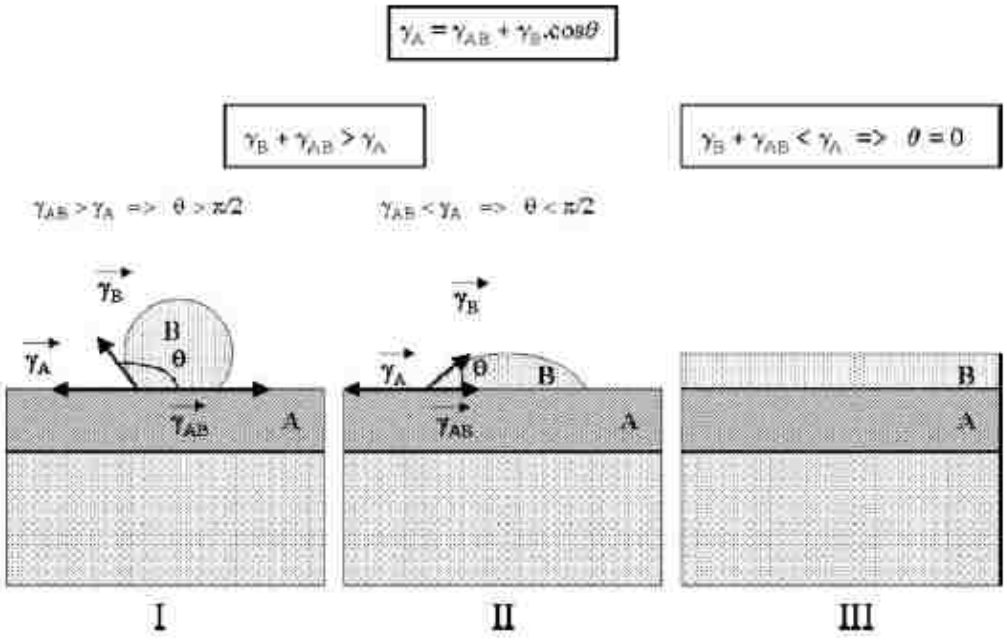

Figure 1.2-4 Illustration of 3 cases of interaction between a liquid deposit (A) and a substrate B: island growth for non-wetting case (I) and wetting case (II) and layer growth for (III) with corresponding conditions of surface energies of the substrate [18]

1.3 Theory of Growth of Carbon Filaments

There are many theories that exist to explain possible growth mechanism of carbon nanofibers (CNFs) which are sometimes referred to as carbon filaments. In general, they may be grown from decomposing a hydrocarbon over relatively hot metal particles (typical diameters between 2 and 10 nm and typical lengths from 5 to 100 μm [19]). The temperature that is needed is generally dependent on the type of metal catalyst used. The

proposed model of the chemical process that occurs during this reaction is that the hydrocarbon is adsorbed and decomposed through certain areas of the metal particle, followed by diffusion of carbon atoms through the metal particle to precipitate at other faces of the particle forming the carbon filaments [6]. This method is commonly referred to as *catalytic carbon nanofiber growth* (CCNF) since the nanosized metal particles act as catalysts for filament growth. It is known that carbon diffusion rate is the crucial parameter in the process [6]. CNFs can also be grown with a variety of chemical vapor deposition (CVD) processes similar to CNTs, but CCNF is generally favored because it allows for large scale production at relatively low cost [18].

Characteristics of the catalyst particles play a tremendous role in the characteristics of the grown filaments. For instance, the catalyst can be found either at the base of the substrate from which the filament is formed, usually encapsulated in carbon shells, or at the tips of the grown CNFs. Figure 1.3-1 shows an illustration of these two scenarios [5]. These two main growth mechanisms are commonly referred to as either base-growth or tip growth.

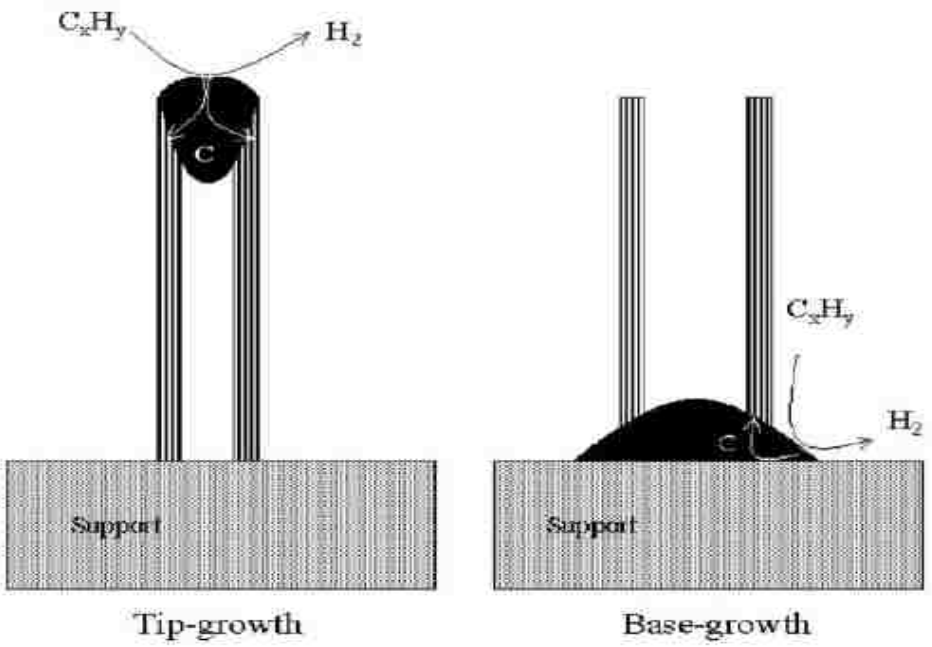

Figure 1.3-1 Two common types of carbon filament growth [18]

Whether tip growth or base growth occurs depends on the interactions between the substrate and the catalyst [6]. There also exists another possibility that the catalyst could end up in the middle of the filament meaning that the filament grew off of two faces of the particle. This scenario is shown in Figure 1.3-2 (a). Tip-based growth is the most common type found in literature but there are cases of base-growth such as CNTs synthesized from FeSi roots under a microwave plasma enhanced chemical vapor deposition (PECVD) [3]. In the published investigations where base-growth occurs, it is speculated that a higher deposition temperature leads to anchoring of the catalyst causing base growth although this has yet to be confirmed.

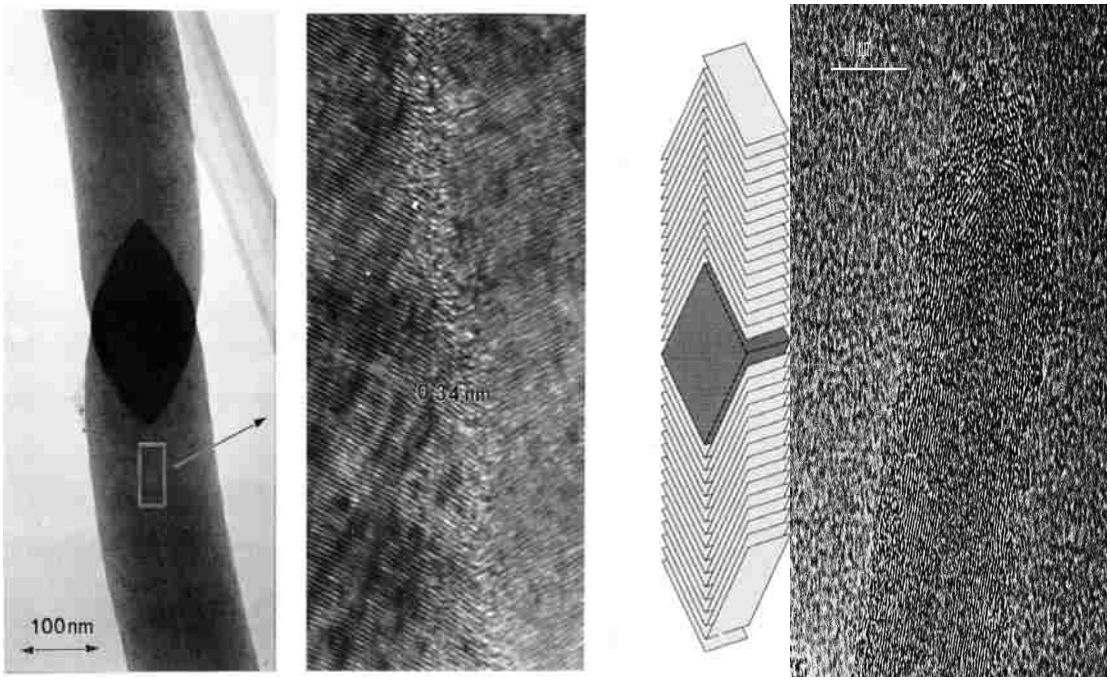

Figure 1.3-2 (a) Electron microscope image of CNF growing in two directions off a catalytic particle. (b) zoomed in image of (a) showing the atomic planes. (c) diagram depicting the atomic planar arrangement shown in parts (a) and (b). (d) electron microscope image of a multi-walled carbon nanotube. [19]

In addition to the final location of the catalytic particle in the filament, the particle's shape also plays a significant role in the morphology of the carbon nanofiber generated whether it be whisker like, branched (multiple whisker like filaments), spiral (like that shown in Figure 1.2-1 (a)), or helical. It is known from basic studies of the interactions between the substrate and catalysts (heterogeneous nucleation) that some planes of the metal particle are more reactive and thus different filament shapes form from the catalyst [20]. The diameter of the catalyst particles determines the growth rate as well as the diameter of the filament itself. Proposed models have also speculated that

there is a minimum diameter of the catalyst which if exceeded will halt growth of any filaments [6].

1.4 Research Objective

Micron scale carbon fibers were chosen as the substrate to synthesize carbon nanofibers with the goal of producing hybrid polymeric composites consisting of multi-scale carbon fibers (nanofiber on micron fiber). It is speculated that including the surface grown CNFs on the composite will act as an interlocking mechanism between the carbon fibers and polymer matrix. A simple analogy is the ridges found on steel rebar which themselves act as an interlocking mechanism between the rebar and concrete matrix. Both short chopped fibers and fibers from a cloth were used in the hopes of producing particulate and reinforced composites respectively.

1.5 Thesis Outline

Due to the vast interest in synthesizing CNFs it would be advantageous to develop a readily scalable inexpensive low temperature process to do just that. Other proposed methods generally involve specialty equipment like vacuum chambers or plasma reactors or require high temperatures (ca. >700°C) where the carbon might become degraded (as a carbon substrate is frequently used). The current thesis proposes the following:

1. To produce CNFs on commercially purchased carbon fibers with Palladium as a catalyst at atmospheric pressure using a temperature of 550°C. Also demonstrate that the process will lead to homogenous distribution of CNFs on the parent fiber and that different carbon fibers (PAN and pitch) may be used as the substrate.

2. Demonstrate a vast improvement in engineering (reducing cost of processes) between the initial amount of Pd loaded on the fiber for the proof of concept and the standard (very low) Pd loading required for homogenous CNF growth. Show the effects of using different protocols (all involving the incipient wetting technique) in loading the Pd in an aqueous solution on the carbon fiber.
3. Varying the parameters of the process to learn the effect of each on CNF generation. By running multiple trials, information will be learned such as: can the metal loading be lowered even further and still lead to CNF generation? Does the distribution of CNFs vary with longer growth times? By obtaining this information one can begin to 'tailor' the process to obtain their desired specimen.
4. Pd will be analyzed using a variety of methods such as x-ray diffraction, transmission electron microscopy (lattice fringe patters), energy dispersive x-ray analysis, and thermogravitational analysis (temperature programmed oxidation). The data form these methods will give information about the degree of crystallinity and composition of the sample.

CHAPTER 2 CARBON FILAMENT GROWTH: STATE OF THE ART.

2.1 Methods of Synthesis for Carbon Nanofilaments on Carbon Fibers

Many groups have grown carbon filaments off a variety of substrates using a variety of deposition methods for the catalysts. The catalysts themselves have also varied although the most popular ones include nickel, cobalt and iron. Chemical vapor deposition (CVD) remains the most common method for growing filaments although three other methods have historical significance and to some extent still used today. These include: arc discharge, laser ablation, and plasma enhanced chemical vapor deposition (PECVD) [8].

Arc discharge process was actually the first process to produce observable multi walled carbon nanotubes (MWCNT) and was followed two years later by laser-ablation which produced single walled carbon nanotubes (SWCNTs) which are much harder to grow [5]. Pryolysis is another method where CNTs and CNFs may be grown which by definition requires high temperatures to decompose a condensed substance [21]. Another common variation of growing CNFs is to grow them in a fluid medium (usually in the gas in the reaction chamber). Catalytic particles are mixed throughout the chamber and allowed to float until they catalyze the reaction. CNFs produced via the fluidizing method are

generally thinner than those produced on a substrate because of shorter reaction times. The floating catalyst method can be used for larger scale production of nanofibers and thus provides potential for several commercial applications.

Generally, most common methods for growing carbon nanotubes have always encountered contamination from other carbon compounds, and methods for separating out the nanotubes so far are not very effective. Currently, selective oxidation method is the leading process to remove impurities from the grown CNTs. Such process can result in losses of ~99 wt.% of the nanotubes [22].

There are several examples of CNFs growth on micron scale carbon fibers. Downs and Baker [23] produced carbon fiber-carbon nano filament structures by impregnating the carbon fibers by an aqueous solution of $Cu(NO_3)_2$ 3H2O and $Ni(NO_3)_26H_20$ salts then flowing an ethylene/ hydrogen mixture over the surface of the impregnated fibers at 600 °C. The process purposed uses oxygen to replace hydrogen and utilizes an intermediate 'activation step' to better disperse the metal nanoparticles that act as a catalyst. It is worth mentioning that there was no variation in the loading of the metal onto the carbon surface which in turn could play a large role in the 'scaling up' of the process into a more commercially viable form.

Thermal CVD has also been employed to grow CNTs on carbon fibers as well. However, with this process it was shown that at 550 ºC the process yielded no growth [24]. More success was observed at much higher temperatures such as 700 ºC. The process itself also

includes an experimental setup where a two zone furnace must be used in which the first zone is kept at high temperature (1000 ºC) and a vacuum is applied via a mechanical pump. Both of these aspects are considerably more costly than the approach being proposed in this thesis (using the proposed method).

Certain gases may be used to grow CNTs on carbon fibers as well. Xylene and Ferrocene have been used in a two stage CVD process with H_2S to synthesize high density multi-walled CNTs on substrates of carbon paper [25]. Iron nanoparticles were first deposited on carbon sheets at a high temperature (900°C) with an m-xylene/ferrocene mixture being fed into a reactor for CVD before a second CVD process was preformed at 1000 °C It was found that adding H_2S greatly increased the deposition of nanoparticles (thus leading to higher density MWCNTs). Based on thermodynamic calculations and electron microscope images, it is speculated that the H_2S decreases the solubility of the carbon in the iron particles thus preventing encapsulation of the particles leading to a high growth rate. While CNTs may have been produced, this process has several limitations. First, very high temperatures are used for this process which can degrade the carbon substrate (in this case sheets of Toray TGP-HO30 carbon paper made from carbon fibers). Secondly, xylene, which is essential for this process, is very hazardous. It has been shown to produce neurological effects such as nausea, dizziness, and drowsiness and is also flammable [26].

Another approach to synthesize MWCNTs entails ohmically heating the metal sites on carbon paper made from carbon fibers [27]. This process involves preparing a silicate gel

and dipping the carbon paper into it and subsequently drying it. A reduction process was then preformed to reduce the nitrates. Then using a reactor where the carbon paper is heated (650 °C or 750 °C) and a 90% Ar, 5% H_2, and 5% ethylene mixture was flown while a current was applied, MWCNTs were grown. It was observed that CNFs rather than CNTs were produced at temperatures lower than 650 °C.

The gel used in this process is made from a mixture of tetraethylorthosilicate (TEOS), ethanol, 2 aqueous solutions of a nickel and cobalt nitrate respectively, and hydrofluoric acid (HF 10%). HF is an extremely hazardous chemical which is corrosive, incompatible with a wide variety of chemicals, and extremely toxic (skin contact may prove fatal) [28]. The process being proposed doesn't use anything as toxic as HF nor a multiple component gel to impregnate the carbon substrate with metal nanoparticles (only an aqueous solution of the metal salt will be used for metal impregnation).

Another popular process for producing multiscale carbon fibers involves synthesizing carbon nanofibers directly on carbon fibers using CVD. One group used type 304 stainless steel (SS) as a catalyst which was applied to bundles of fibers using sputtering [29]. After the application of the catalyst a reduction heat treatment was implemented by flowing diluted hydrogen (N_2/H_2) at 660°C. For CNFs growth, the hydrocarbon flowed was acetylene (C_2H_2) for ½ hour at the same temperature of 660°C. For the GSD protocol to be adapted later, the temperature does not need to reach this range to grow CNFs.
It was shown that by using the CVD process carbon nanotubes are grown on the carbon fibers (thickness of 250-550 nm surrounding parent fiber). Single fiber composite

specimens were prepared and using a micro tensile test it was shown that the addition of nanotubes to the surface of the carbon fiber in the matrix results in a 15% improvement in the interfacial strength as compared to a composite sample with a bare carbon fiber.

Another group preformed CVD on carbon substrates (including unidirectional and bi-directional carbon fiber tows) to grow CNTs and then used a three point flexural loading test (using Instron universal testing machine) to determine mechanical properties of a composite with the 'multi-scale' carbon fibers [30]. Using this test it was shown that an improvement in flexural strength of ~20% was achieved when the carbon fibers with CNTs were used to replace the ordinary carbon fibers, with no nanofilaments, in the composite. The CVD process for growing the CNTs comprised of heating the sample up to 750°C and the use of a mixture of ferrocene and toluene as the reactant gases to form the hydrocarbon (in conjunction with iron previously deposited on the fiber). Once again a relatively high temperature was needed in the process to grow CNTs.

CVD processes have also provided information about the nature of the catalyst in regards to the diameter of the CNFs (in this case CNTs) synthesized. Through the CVD treatment on graphite foil, that was coated with stainless steel film via sputtering, it was observed through TEM that the outer diameter of the CNT increased with increasing the thickness of the catalytic SS laid down while the inner diameter of the CNT did not increase after reaching a maximum value of ~ 7 nm [31]. It was concluded from that research that CNTs can not form on catalyst particles that are too small at a low reaction temperature because they will not reach the energy needed for nucleation to occur.

Similar to the GSD process being proposed to grow CNFs, the growth step took place in a tube furnace with a mixture of acetylene, C_2H_2, (at 10 sccm) and N_2 (at 100 sccm) flowing at a temperature of 660°C for 1 hour. However unlike the GSD process, the pressure in the chamber was not atmospheric (it was at 0.3 Torr).

The general drawback of using CVD to synthesize CNTs/CNFs is that the process requires elevated temperatures (above 650° C) to ensure the growth. Also vacuum is required in most CVD cases. Furthermore, CVD requires specialty equipment (deposition chamber, pump, etc.) which are not necessary in the operating conditions of the GSD process being proposed which uses an ordinary tube furnace and standard laboratory equipment. While the improvement in mechanical properties of CNT on carbon fiber composites (synthesized by CVD) is significant it is postulated that similar effects could seen on CNF-on-carbon fiber composites that can be processed at lower temperatures under simpler more cost effective operating conditions; namely the graphitic structures by design process.

2.2 Graphitic Structures by Design (GSD)

This combustion process is based on the recently developed 'Graphitic Structures by Design' (GSD) process[32]. By using the unique characteristics of the GSD approach (relatively low temperature, standard atmospheric pressure), a theoretical assumption of prior work is challenged which is that synthesis of carbon nanofibers (nanotubes or otherwise) occurs due to thermal decomposition of molecules. Furthermore, a new theory

is formulated that the actual driving force of nanofiber synthesis is the creation of radical species created by the combustion process.

Phillips et al. [32] showed that different graphitic structures can be grown at different conditions and thus graphitic structures can be grown 'by design'. For instance, two of the main conditions that can be varied are the temperature and the fuel mixture used during deposition via a hydrocarbon combustion process. Figure 2.2-1 shows the different morphologies produced by varying these two conditions (using nickel nanoparticles). Interestingly filaments were found to form at low temperatures during the process. At higher temperatures, using Ni, only graphite that mimicked the shape of the template referred to as graphite template, formed.

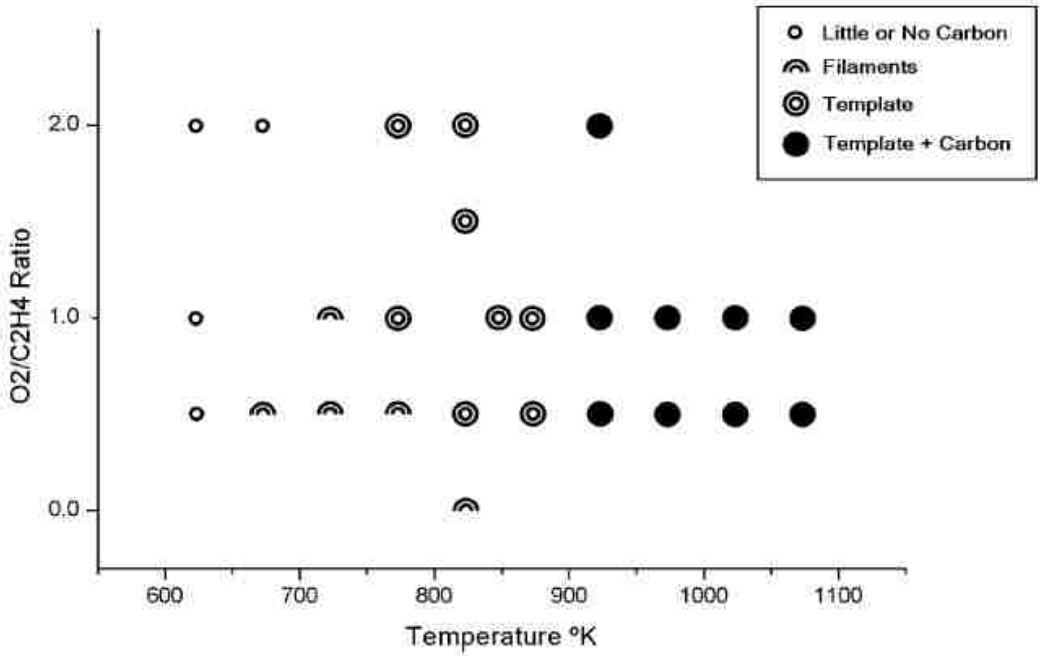

Figure 2.2-1 Different Morphologies resulting from varying environment of Nickel nanoparticles [32]

Phillips et al. [32] used a simple quartz tube furnace for their experiments. They found that the relative position of the sample in the furnace during the GSD process greatly affects which morphological type of carbon is grown, if any. For instance, during a deposition at 550 °C on 2 pieces of graphite lattice which were placed 7 cm apart in the same furnace, it was observed that the piece placed in the center of the tube (directly near the heating element) had deposits of graphite while the other sample that was placed 7 cm further into the tube (from the inlet where the gases entered the chamber) showed no growth. This can be seen in Figure 2.2-2.

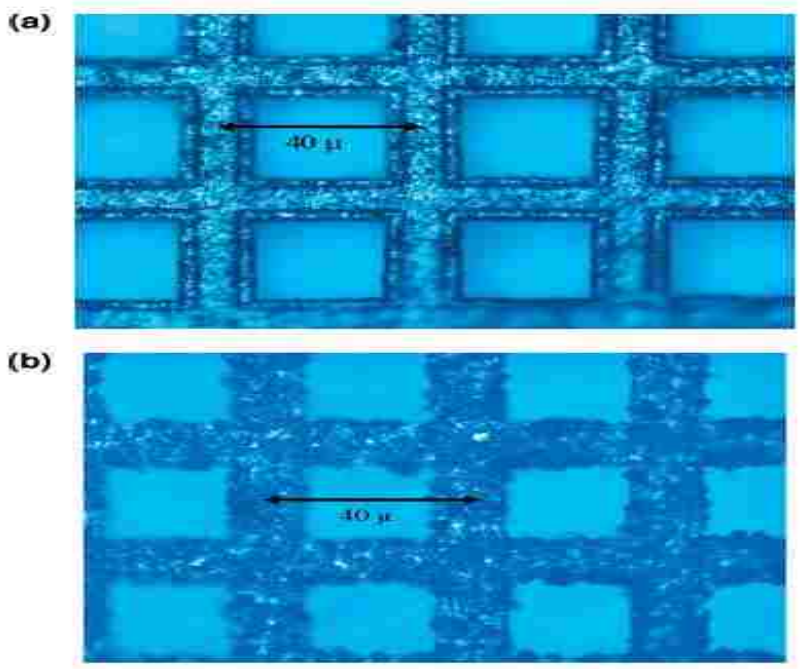

Figure 2.2-2 Illustration of importance of placement of sample during deposition in the GSD process (a) shows graphite lattice placed 7 cm upstream form the heating element while (b) shows a graphite lattice samples that was directly underneath the heating element during the GSD process [32]

The investigators used 3 different types of metal catalysts for their experiments: nickel, iron and aluminum. Aluminum is typically not used as a potential catalyst in filament synthesis because it is not a transition metal (like nickel, iron and cobalt which are all popular catalysts). Here in the GSD process it lead to no growth of filaments while undergoing the same operating conditions that had been used on the Ni. Nickel was the primary metal catalyst used and observed to have a growth rate of about 1 graphite layer/s. Iron produced carbon growth but at a slower rate then Ni.

The x-ray diffraction (XRD) studies employed by Phillips et al. [32] showed that the carbon structures grown are graphitic. Also, it was shown that an acid treatment could be used to remove the metal catalytic particles to produce XRD results without dominant Ni peaks thus leaving the character of the actual carbon as the subject of interest

CHAPTER 3: USE OF PALLADIUM AS CATALYST FOR NANOFIBER GROWTH

3.1 *Experimental: Standard Protocol*

The combustion process consists of four main steps. Note that all of these steps are accomplished with basic laboratory equipment (small furnace, gas bottles, etc.) unlike some of the methods discussed earlier [3] and at temperatures (c.a. 550° C) where there is no chance of carbon degradation which can not be said of methods involving CVD. [4]. The steps are as follows: (i) removal of the sizing off of the surface of the carbon fiber, (ii) 'activation by burning' to form nucleation sites for a metal catalyst to adhere to, (iii) loading of the metal catalyst onto the carbon fiber, and decomposition of the metal salt byproducts, and finally (iv) growth of the carbon fibers via the metal catalyst.

The main furnace (one-zone) used for experiments is a Lindberg Hevi-Duty furnace that measures 12 inches long with a heating element in the center. Four gas tanks were used for this process: reduced hydrogen: N_2H_2 (90:10, N: H), N_2, C_2H_4 and O_2. The gas flow rates were controlled by four mass flow controllers (MKS Vacuum Gauge and Measurement System Type 146). The sample holder is a sintered alumina boat into which the carbon fibers were placed. The gases were exhausted out through an exhaust hood. Figure 3.1-1 shows a schematic of the setup.

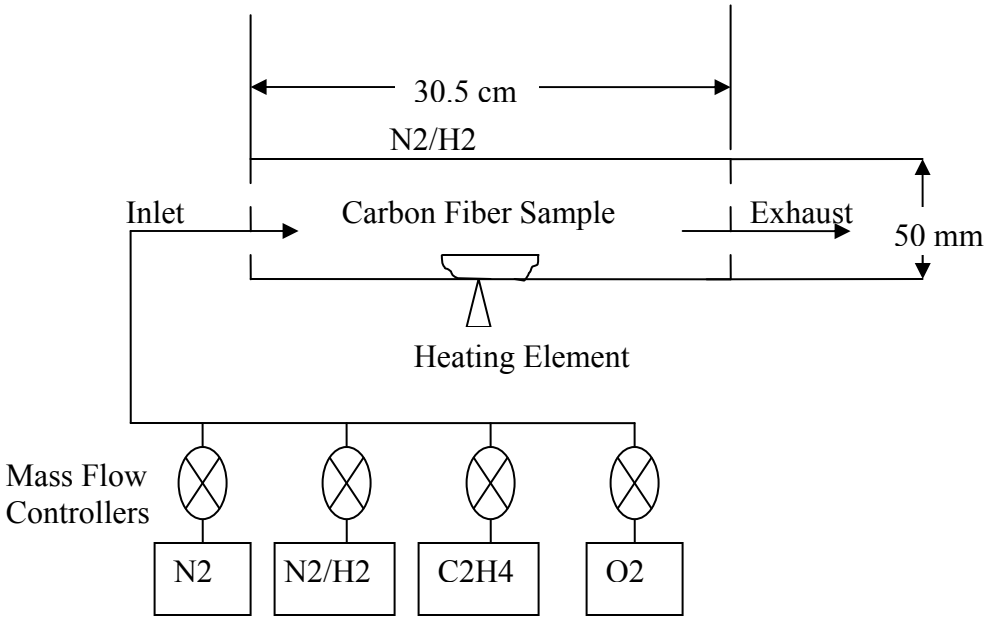

Figure 3.1-1 Schematic of chamber used in Lindberg Hevi-Duty® furnace

The temperature profile inside the chamber is important due to the influence of temperature on nanofiber synthesis. Therefore, the temperature was mapped throughout the chamber via a thermocouple probe while N_2 was running at 600 standard centimeters cubed per second (sccm) as shown in Figure 3.1-2. The largest difference between the actual and nominal temperatures (~75-85% of nominal value) can be seen to occur closer to the inlet. The middle of the chamber is where the actual values are the closest to the nominal values (~50°-70° C difference). Close to the gas inlet the temperatures begin to vary greatly from nominal values in a similar fashion as what was seen near the outlet. Experimentally, the large temperature gradient across the chamber was taken into account by placing multiple samples inside the chamber during some experiments to note its effect.

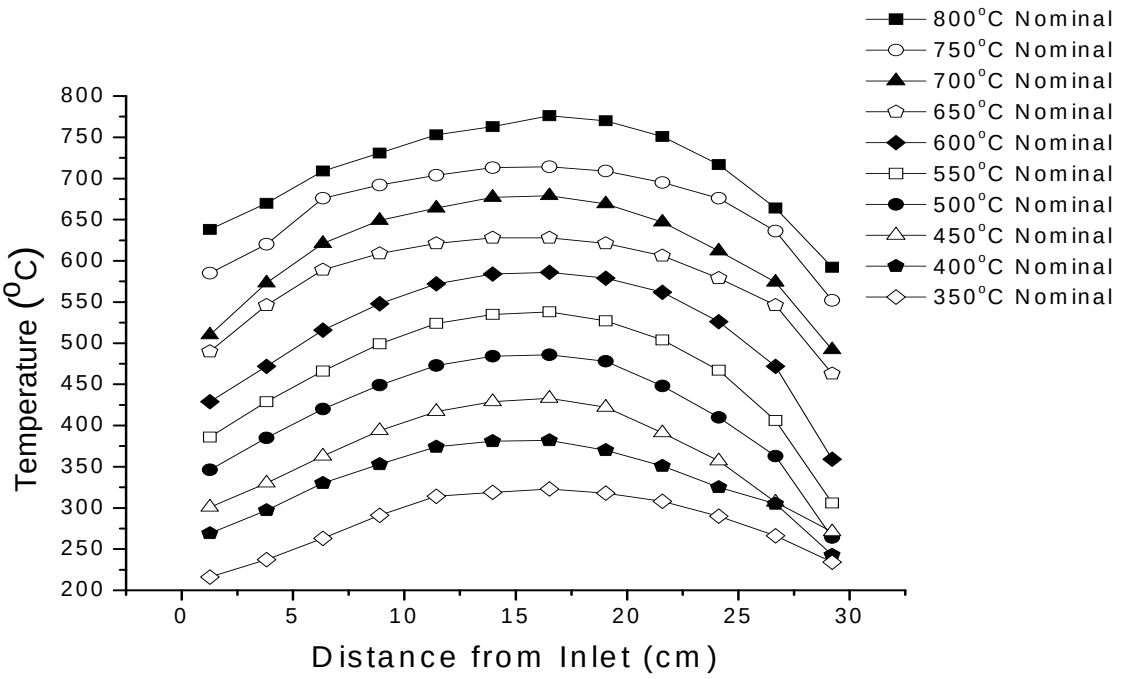

Figure 3.1-2 Temperature profile of Lindberg Hevi-Duty® furnace [33]

The Lindberg Blue-M furnace that was used during later experiments is a three zone furnace meaning that each 'zone' has its own temperature PID controller as shown in the schematic of Figure 3.1-3. A 36" long quartz tube was used where one has the ability to use 3 zones simultaneously for experiments.

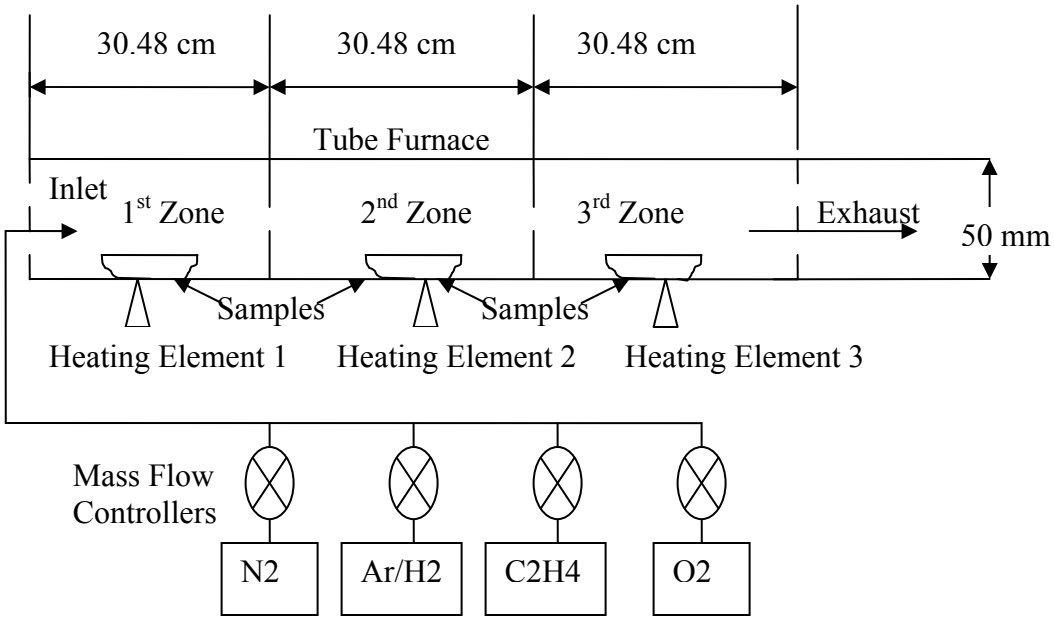

Figure 3.1-3 Schematic of 'long' chamber used in Lindberg Blue M furnace; the 'short' chamber utilized only zone 1 for heating

Figure 3.1-4 shows a temperature along the first zone of the Blue M furnace (as if the 16" long tube is being used as the chamber. It is presumed that the second and last zones will have similar profiles due to the lengths of the zones being equal and that one heating element is located in the middle of each of them. Measurements were taken with a thermocouple attached to a digital thermometer while N_2 was flowed at 300 sccm. Similar to the profile of the Hevi-Duty® furnace, there is a large temperature gradient across the span measured. However the difference between the closest temperature measured and the nominal temperature is far greater for the Blue M furnace (as high as 38% of the nominal value). Therefore to achieve a desired temperature in the furnace the temperature on the controller was set to the calibration curve shown to give the desired temperature directly by the heating element (in the middle).

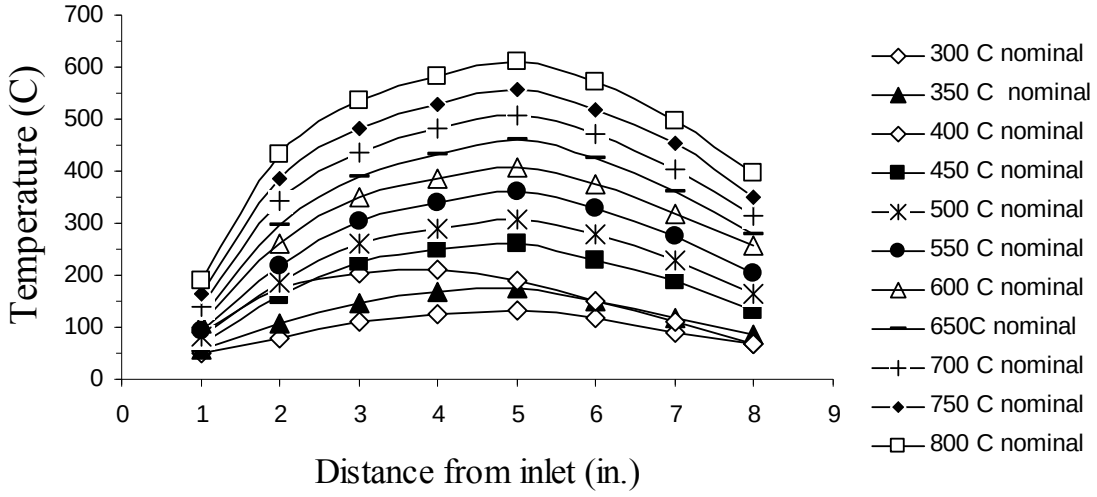

Figure 3.1-4 Temperature profile of Lindberg Blue M furnace

3.2 *Substrates for Growth*

All carbon fibers start with a precursor fiber and the two main types of precursors used today are polyacrylonitril (PAN) precursor and pitch as a precursor. PAN is the most widely used precursor today. All PAN precursors are acrylic based and contain at least 85 percent of acrylonitrile but the secondary polymers are trade secrets which offer slight improvements in some properties [34]. Raw pitch comes from the distillation of residual oils from crude oil. These oils are heated to temperatures between 350°C and 500°C which results in heavier material with higher carbon content that forms the basis of the pitch fiber precursor.

Both types of precursors have their own advantages and disadvantages. Pitch-derived fibers offer higher yields and faster production rates (due to graphitization times on the order of a few minutes) but they are more brittle than PAN based fibers and have lower

specific properties (due to a higher density). The microstructure of the fibers is also different: a cross-section of a pitch based carbon fiber is perfectly circular while that of a PAN based fiber is only slightly circular [34].

For the sake of robustness of the process both PAN based and pitch based carbon fibers were used with the GSD process. PAN based short chopped carbon fibers (3 and 6 mm length) were commercially bought from Toho Tenax America, Inc. with an approximate diameter of 7.5 μm. Figure 3.2-1 shows a scanning electron micrograph shows what a short PAN fiber looks like. One can see from the micrograph that the surface of the 'as-received' carbon fiber is rather unremarkable and bare. Long PAN based long (c.a. 12-15" in length) carbon fibers were purchased from Grafil Incorporated.

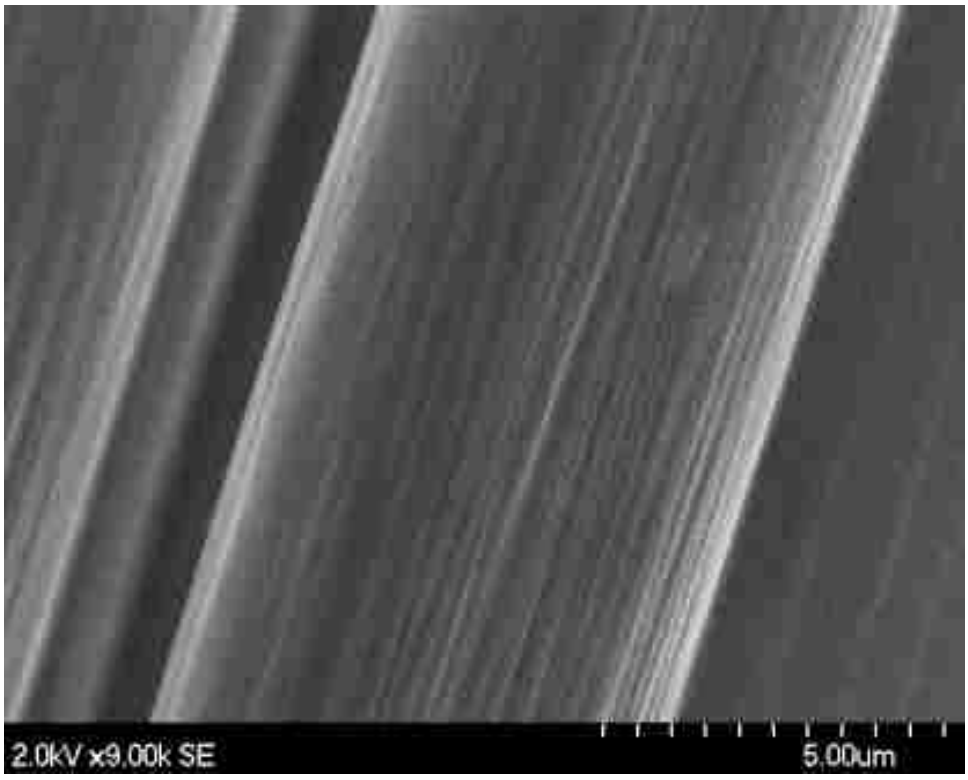

Figure 3.2-1 Scanning Electron Micrograph of short chopped PAN carbon fiber as received from manufacturer

Thornel® Carbon Cloth VCD-20 continuous Pitch-based Carbon Fibers were obtained from Cytec Industries Inc The average diameter of these fibers is around 8 microns and they obtain higher density, dramatically higher thermal conductivity, more negative CTE, higher modulus, and superior frictional characteristics compared to PAN-based fibers.

3.3 *Removal of the Sizing*

Removal of the sizing off the carbon fibers substrates is needed to expose the actual surface of the carbon fiber. Sizing is a thin polymer coating, required for health reasons to prevent any inhalation of carbonaceous material, which manufacturers put on carbon fibers (note: no carbon fiber without the sizing is available commercially). The exact composition of the sizing on the carbon fibers is a trade secret although examples of sizing include polyvinyl alcohol (PVA) and polyvinyl acetate (PVAc) [35]. Along with being required for health reasons, the sizing is placed on carbon fibers is to prevent the carbon fibers from contact damage (either from themselves or equipment nearby during pre-impregnating) when they are on the tow (which can consist of 12000 fibers or more). Because sizing is mostly polymer based it does not dissolve in water and thus requires a heat treatment in order to remove.

Removing the sizing consists of two steps. First, a heat treatment is preformed in oxygen-rich environment flowing at 100 (sccm) under 525 °C for 10 minutes to decompose the sizing. This temperature is lower than that of other procedures where 700°C is used while the sample is also in a vacuum chamber [29]. The second step involves the following: soaking the fiber for 1 hour in acetone in an air tight container to

dissolve the sizing off of the fibers, rinsing the acetone off the fibers with ethyl alcohol on a sieve, and finally drying in air for 1 hour at 100 °C.

3.4 *Activation by Burning Pretreatment*

The second part of the process is a novel step not used before for nanofiber on fiber growth. It involves a heat treatment in oxygen for 20 minutes at 525 °C. Recall that during this step the fibers are relatively free of sizing which means that a small amount of the carbon fiber (c.a. between 5% and 10% weight loss) will be burned off during this step. Via this burning, it is theorized that oxygen groups are formed which serve as nucleation sites (more hydrophilic) for the metal to be deposited in the next step. This is supported by research which shows that having residual gases before or after nucleation and growth (in this case metal nanoparticles) influences the morphology of the particles. It has been found that using vacuum pressures results in unoriented particles (particularly for Palladium) while using higher pressure results in more oriented uniform particles [36].

3.5 *Impregnation of Catalyst via Incipient Wetting*

After the burning treatment, the parent fiber is impregnated with the catalytic metal via the incipient wetness technique. Other methods such as sputtering and electrochemical deposition can be used to deposit the metal but incipient wetness offers a process which does not involve any specialty equipment and has been shown to be effective even with very low net metal loadings (0.5 wt. % Pd: C).

The process entails making an incipient wetness solution (IWS) of distilled water and the metal salt (in this case 99.9% Palladium (II) Nitrate hydrate from Sigma Aldrich). An incipient wetness ratio defined as the amount of water just needed to saturate a known amount of fibers is used to determine how much distilled water is used using an assumed amount of carbon fiber. Note that this is not the actual amount of carbon fiber that will be loaded with the metal, but it is an amount greater than the actual amount to prevent the experimenter from having to weigh an unreasonably low amount of the metal salt (<2 mg) accurately.

After the amount of distilled water is determined, the amount of metal salt to mix with the water is determined by the net metal loading percent which translates to a ratio of the amount of the metal (Palladium) to the assumed amount of carbon fibers. Palladium is an interesting metal to be used as a catalyst as the contact between nanofibers and the Pd after nanofibers or CNTs is ohmic in nature meaning unlike other metal catalysts, it would not disturb the electrical transport properties of CNTs [18]. It is also a noble metal and traditionally transition metals are used as sole catalysts in CNFs/CNTs synthesis.

Since a metal salt and not the pure metal is used in the experiment, a ratio of formula weights between the metal salt and the actual metal (e.g. Palladium (II) Nitrate Hydrate and the Palladium) is used to convert to the amount of metal salt in the IWS. After the metal salt is poured into the distilled water, the solution is sonicated to produce the homogenous IWS. Then a portion of the IWS (determined by the ratio of the actual amount of carbon fiber to the assumed amount of carbon fiber) is put into a syringe and

the carbon fibers are saturated drop-by-drop on a watch glass. The solution is then evaporated in air at 100 °C overnight to leave the fibers with a form of the metal (mixed oxide) for the deposition. A calcining treatment (30 minutes in an inert gas at 106 sccm followed by 4 hours at 250 °C in the inert gas) is then used to decompose the metal salts further.

It has been shown that pretreatment steps prior to actual growth conditions has a dramatic impact on the yield of CNFs produced and can even dictate if CNFs are grown at all [37]. These steps affect the conditions of the catalytic metal nanoparticles during growth (size of filaments, if filaments can be produced). Therefore it is important to monitor these effects in the design of a protocol to grow CNFs.

3.6 *Growth Step: Filament Generation*

The growth step, the final step in the process, actually consists of 4 sub steps as utilized by the GSD process. The first sub step consists of simultaneously flowing an inert gas for 20 minutes while heating up the furnace to 550 °C. This purges any air from the quartz tube in the furnace. Then a reduction takes place in diluted hydrogen for 1 hour at 550 °C to reduce the already calcined metal particles further to pure Palladium. Then another purge in an inert gas is preformed for one hour to rid the chamber of the diluted hydrogen. Finally the last sub step is preformed which chemically causes the filaments or nanofibers to form off of the carbon fiber. This step is termed the deposition and is accomplished by flowing oxygen (O_2) and ethylene (C_2H_4) at low amounts (15 sccm) while also flowing an inert gas at a higher amount of Nitrogen (N_2 at 300 sccm) to keep

the system diluted. The time of growth is varied in order to produce different lengths of filaments.

The thermal decomposition model does not quite fit the experiments preformed with the combustion process. If thermal decomposition is the growth mechanism of carbon nanofibers (CNT and otherwise), it is reasonable to assume that changing the time of the 'activation' burn would have no effect on nanofiber growth. Yet the opposite was shown to be true. It has also been shown that oxidation can be used to grow carbon nanofibers at a lower temperature than other methods even with a supposed 'poor' catalyst such as Palladium. Therefore, the formation of radicals needs to be included in the discussion of growth mechanisms as an aid to nanofiber growth. It has been shown in this research to clearly be a factor.

3.7 Variations of Sizing Removal

To remove the sizing coating off the carbon fibers, various trials were utilized to ensure that the entire surface of the carbon fiber would be available for processing. First it was needed to be seen if burning the carbon fiber by itself would be satisfactory to remove the sizing. This procedure was preformed at 500 °C in oxygen for 1 hour on short chopped PAN based carbon fibers. The furnace used for this experiment was an Applied Test Systems short quartz tube furnace. The results of simply heat treating the sample to remove the sizing can be seen in Figure 3.7-1 via a scanning electron micrograph. A JEOL-5800LV microscope was used for taking the micrograph. It is apparent that flakes of debris (c.a. 1-2.5 μm) remain on the sample. The weight loss for this sample after the

heating treatment was 19%. Initial speculation was that a high amount of weight loss of the carbon fiber would be needed to form nucleation sites for deposition of the catalyst.

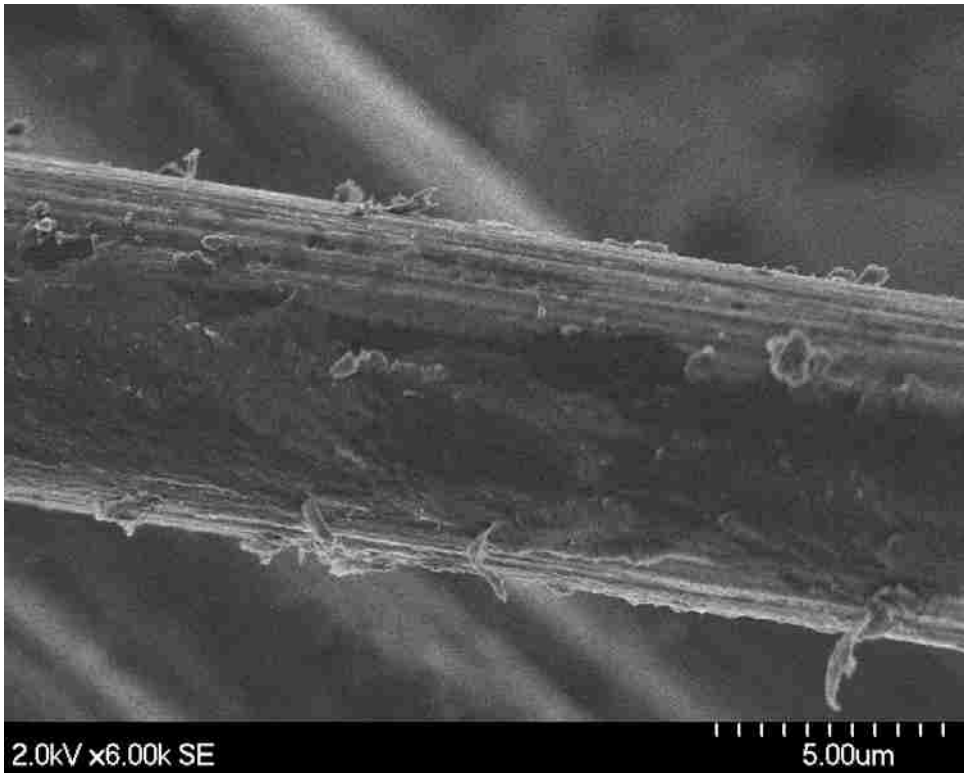

Figure 3.7-1 Results of heat treatment only (500° C in O_2) in removing the sizing

Energy Dispersive Analysis (EDS) was used to try to characterize the debris further. The scanning electron microscope that had been used for the micrographs was also equipped with EDS and PGT spirit software for analysis of the EDS data. The spot analysis technique where analysis is preformed on one spot at a time on the sample, was used for data analysis. Three spots were analyzed (2 of which were large pieces of debris while another was small) in order to try to get representative data. Figure 3.7-2 shows the micrograph of the area where spot analysis was preformed (along with the 3 locations used) and Figure 3.7-3 shows the spectrums from each spot. From this figure, it can be seen that the dominant peak is carbon which has a much higher relative intensity than the

peak for oxygen. Interestingly, no peak was observed that indicates a polymer character for the regions scanned.

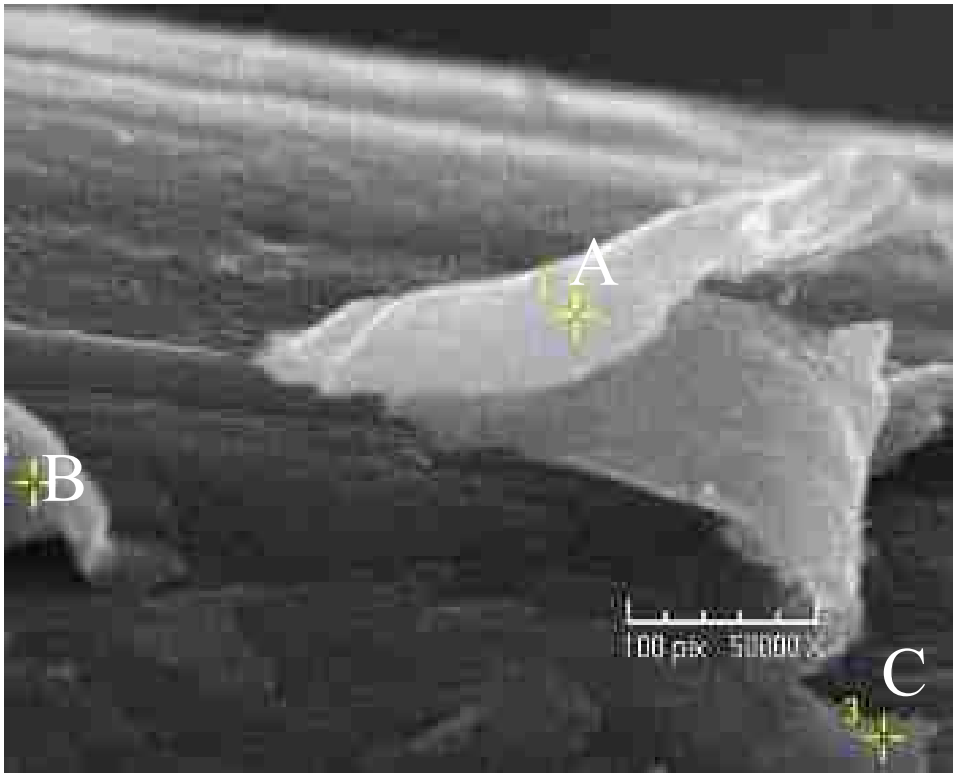

Figure 3.7-2 Micrograph of sample for corresponding locations (A, B, and C) analyzed under EDS (spot analysis) whose spectrums are shown in Figure 3.7-3

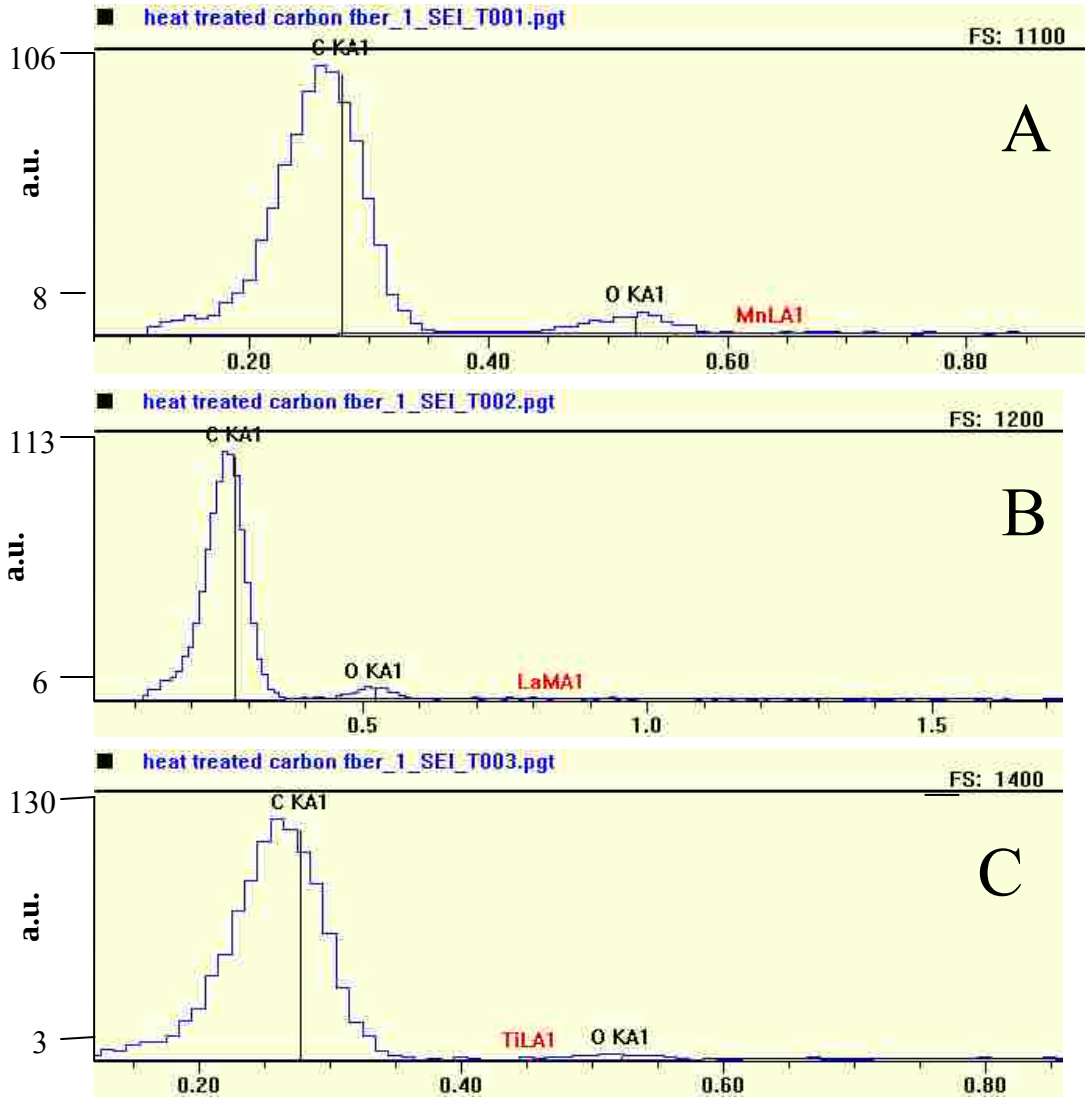

Figure 3.7-3 EDS analysis of sample after heat treatment (A, B, and C represent the spectrums of each respective location); y-axis is arbitrary units (counts)

After it was observed that heat treating the sample was not efficient enough in removing the sizing, a rinsing procedure was applied to the sample. Various trials were applied to the fiber using both an ethanol only and ethanol and acetone rinses. It was observed that the best results were reached with a procedure involving using acetone and ethanol to

remove the sizing. The role of the ethanol is to remove acetone that is left on the carbon fiber surface. Acetone breaks up the sizing which was observed to appear as a solid substance floating on top of the left over acetone after the fibers had been sitting with the acetone in an air tight container for a significant amount of time (>1 ½ hour). Figure 3.7-4 shows the best results reached when the standard procedure described in section 2.3 was followed.

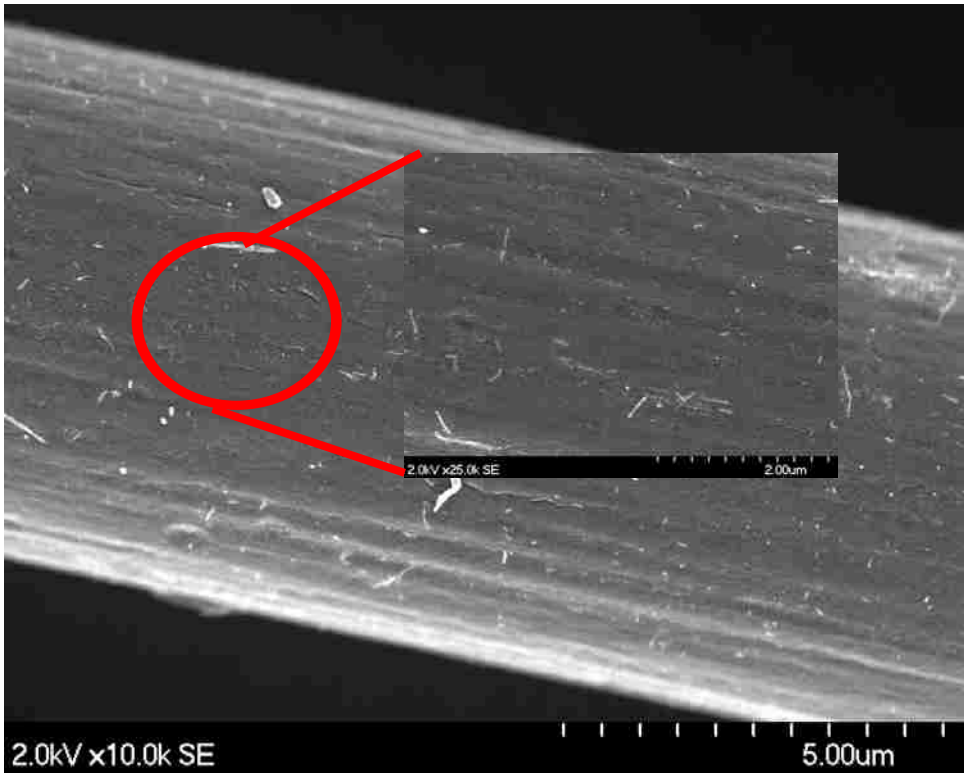

Figure 3.7-4 Results of heat treatment and rinsing in removing the sizing

One minor modification that was made to the sizing removal protocol (implemented with the pitch based carbon fibers and the long PAN based carbon fibers) was in the step where the polymer sizing is removed off the surface of the carbon fiber. Previously the step involved burning the sizing in an O_2 environment and then washing away the residual of the sizing from the carbon fiber surface by soaking the fibers in acetone and

rising in ethyl alcohol. While the rinsing step remained unchanged, the burning of sizing for the Ni protocol samples was preformed in air in a Lindberg furnace using the temperature profile shown in Figure 3.7-5. Since no noticeable difference in the effectiveness of removing the sizing between the two burning steps (with and without O_2) could be seen under electron microscopy, the non-O_2 heating treatment was adopted as part of the standard protocol for the sake of added simplicity of removing the need to flow a gas during a step.

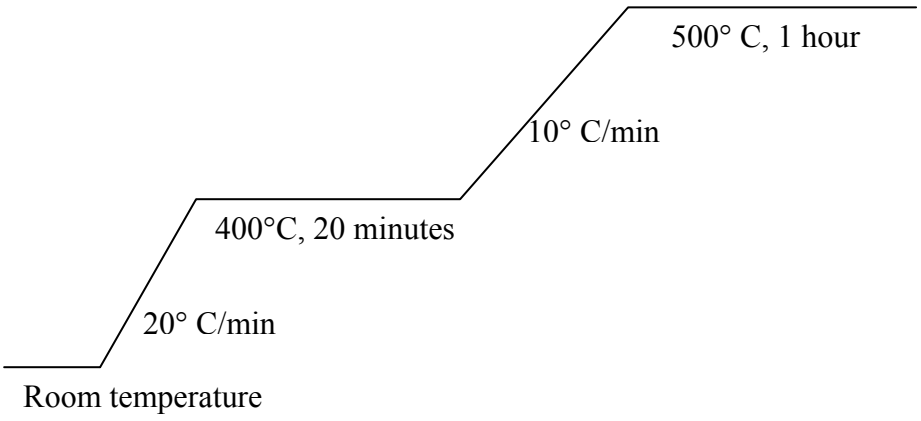

Figure 3.7-5 Temperature Profile used to burn sizing in air

3.8 Initial Trials of Incipient wetting and Proof of Concept

Initially, it was not known how much solution would be needed to impregnate the sizing-free carbon fibers in order to achieve the growth of CNFs. An initial incipient wetness solution (IWS) was made and consisted of 15 mL of distilled water, 5 mL of isopropyl alcohol, and an amount of crushed Palladium (II) nitrate hydrate salt. Three different

loading rates of the metal catalyst (Palladium to Carbon) were used to determine what amount was appropriate (after inspection afterward). They were: 467% loading rate, 326% and 185%. The amount of short chopped PAN carbon fibers used for the experiment was ~18.6 mg; therefore the actual amount of metal salt used for the initial trials was 166 mg, 116 mg, and 66 mg; respectively. The procedure for the first trials of incipient wetting was as follows: the fibers were pretreated in a quartz tube furnace for 2 hours at 450 °C under O_2 (flowing at 162 sccm), then the fibers were placed in a beaker and 5 mL of the IWS was added, the sample was then placed on a hot plate (with agitation via a magnetic stirring rod) until the solution evaporated. This procedure was repeated 3 times until all the IWS had been used up. Afterward, the fibers were dried overnight in a small oven at 100 °C. Figure 3.8-1 shows scanning electron micrographs from all three samples of the initial trials.

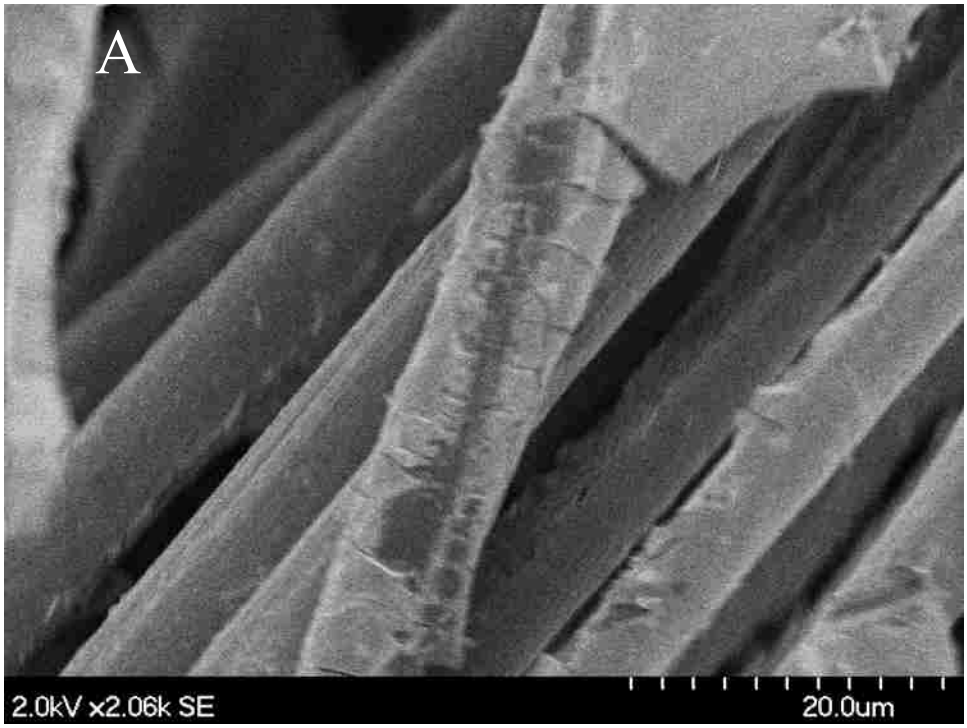

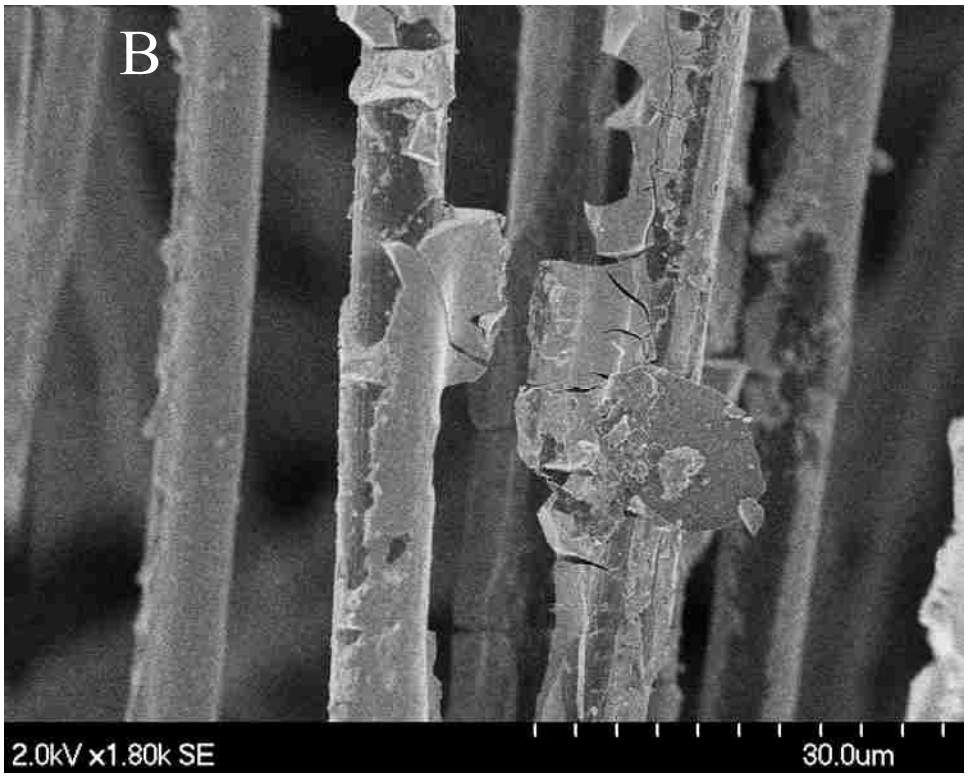

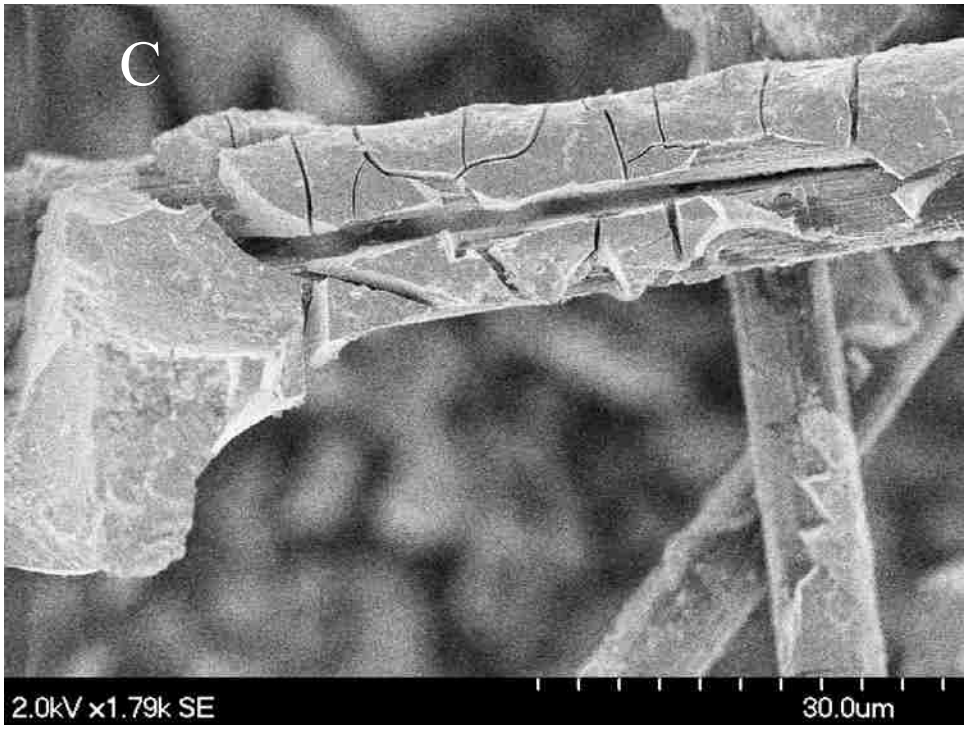

Figure 3.8-1 Sample after initial trials of incipient wetting (a) 185 % Pd loading (b) 326 % Pd loading (c) 467% Pd loading

It can be seen the initial loadings resulted in the fibers being encased in the metal. In other words, metal nanoparticles are not generated. Because of this result, the metal loading was reduced to 37.2%, 19.4% and 5.63 % respectively. The amounts were based on using at most one fifth of the previous smallest concentration. The same procedure as for the initial trials was repeated for the sample. Scanning electron micrographs were once again taken for the three samples. From the micrographs it was clear that the lower concentrations resulted in two distinct morphologies of the metal being formed. Figure 3.8-2 shows that the two morphologies are small spherical metal nanoparticles (c.a. 5-10 nm in diameter) and larger agglomerations of the metal. Both morphologies generated are smaller than the encasings of the earlier trials. As a result of the agglomeration observed, it was concluded that the metal catalyst was not distributed evenly over the surface of the carbon fiber and thus a new protocol for incipient wetting was needed. Also from both sets to trials used (higher and lower loadings) it was observed that the metal loading could be lowered even further.

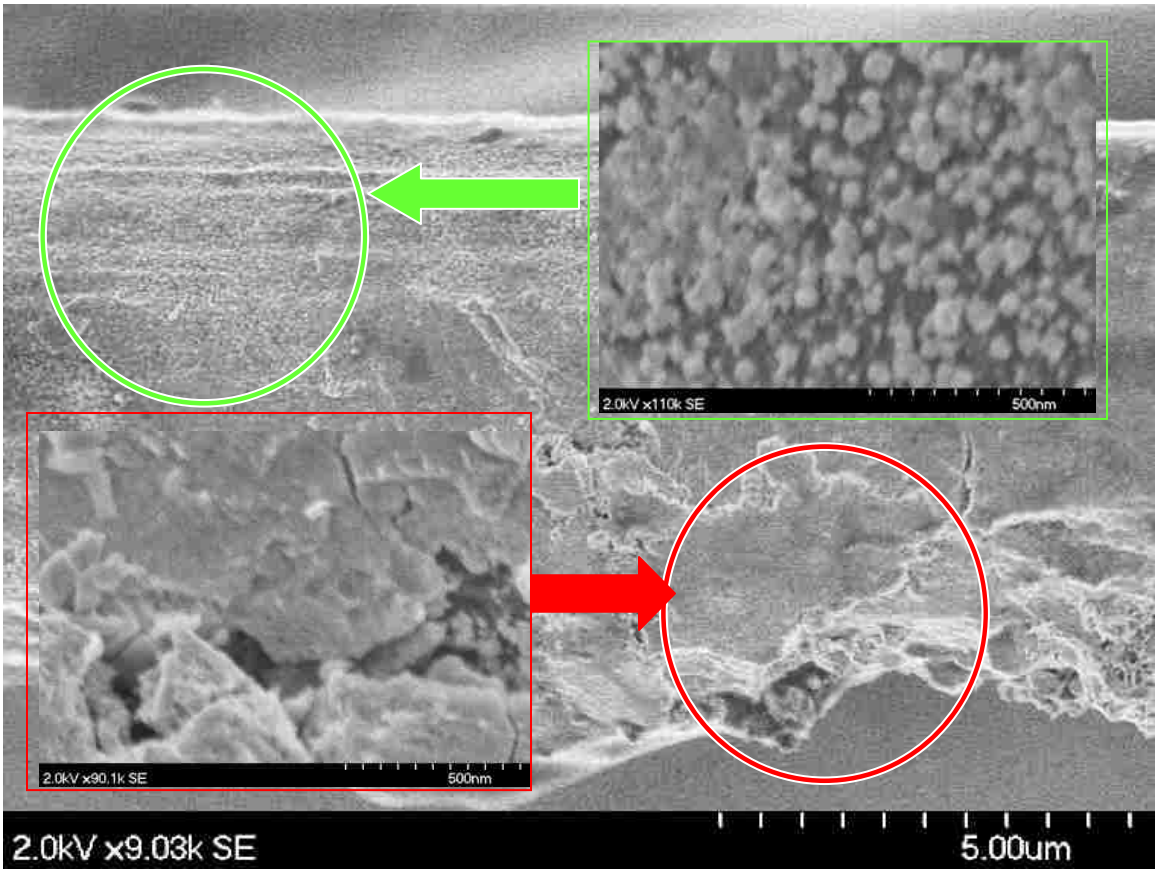

Figure 3.8-2 Sample after incipient wetting (19.4 % Pd loading) showing 2 morphologies of Pd deposited

A new method for incipient wetting was explored in order to generate a more uniform coating of the catalyst. For this method of incipient wetting the IWS consisted of 15 mL of isopropyl alcohol and 5 mL of distilled water as before, but this time 1% metal loading (2 mg of Palladium (II) Nitrate hydrate for 90 mg of short chopped PAN carbon fibers) was used. For this method the effect of sonication was explored. Two experiment setups were employed. Figure 3.8-3 shows the setups used for sonication and without sonication.

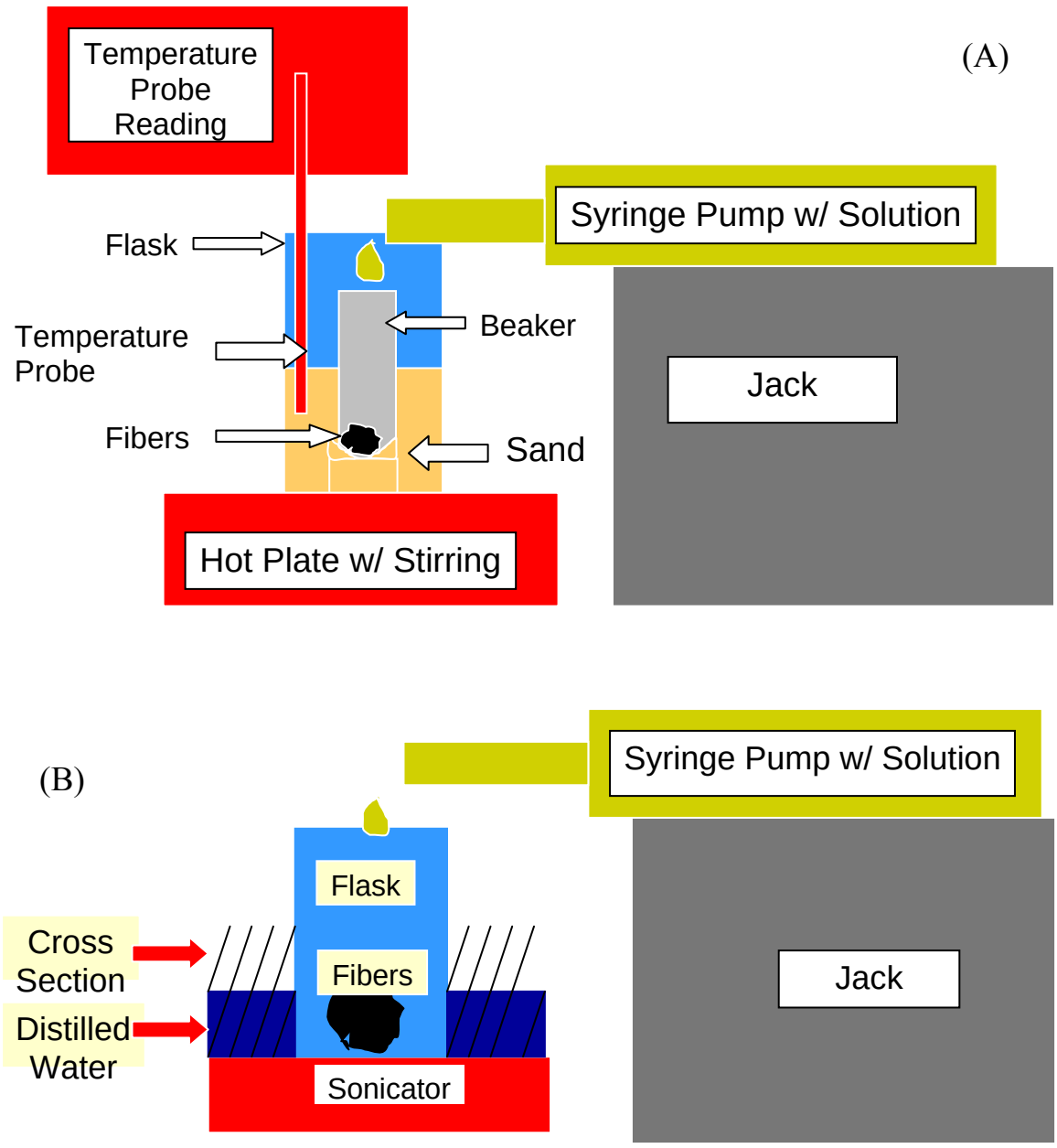

Figure 3.8-3 Two setups used for the incipient wetting technique (a) employs no sonication while (b) uses sonication

For these trials a syringe pump was used to dispense the 20 mL of IWS 'drop by drop'. It was speculated that having one drop of the solution dispensed at a time (while the sample was being agitated either by ultrasounds or by stirring) would result in a more uniform

distribution of the catalyst on the carbon fiber substrate. The hotplate used for the procedure without sonication had a temperature probe which was inserted into sand that covered the walls of the beakers that the carbon fibers were placed in. This was done with the idea that the sand would heat the walls of the beaker uniformly and thus result in more uniform deposition of the catalyst salt. A magnetic stirring rod was also placed in the beaker for the sakes of agitating the sample. The temperature used for evaporation was relatively low (~87 °C). The problem observed for the non-sonication method was that the evaporation times varied greatly in 2 runs of the procedure. One run took about 2 hours to evaporate while the other took 11.5 hours for the solution to evaporate fully. More runs would be needed to analyze statistics of the runs although experimental error may have come into affect with other conditions such as the quality of the isopropyl alcohol used, environmental temperature conditions, etc. The sonication method involved using a Branson 2510 ultrasonic cleaner to agitate the carbon fibers. Distilled water was used as the medium for the ultrasound waves to pass through as the ultrasonic cleaner was filled about one-third with it.

After both samples (sonicated and non-sonicated) underwent 'drop-by-drop' incipient wetting via the syringe pump the samples underwent a reduction heat treatment for 3 hours under N_2/H_2 gas (204 sccm) at 400 °C in order to decompose the nitrates of the salt. Then both samples underwent the following GSD protocol using the Lindberg Hevi-Duty furnace: N_2 was flowed at 100 sccm for 20 minutes to purge the chamber, reduction was preformed with reduced hydrogen (90:10 Ar:H_2) at 50 sccm for 20 minutes, N_2 was flowed again at 600 sccm for 20 minutes to purge the chamber from the hydrogen. The

difference between the samples was the time of the 'growth' or deposition of the hydrocarbon. C_2H_4 and O_2 were flowed simultaneously at 15 sccm each (along with N_2 at 300 sccm to keep the combustion mixture dilute) for either 1 minute or 5 minutes. Figure 3.8-4 shows the scanning electron micrographs of the samples (non-sonicated and sonicated) after one minute deposition and Figure 2.8-5 shows the micrograph of the sonicated sample after 5 minute deposition. Note that after it was observed that the non-sonicated did not produce any carbon nanofibers after one minute, no 5 minute deposition was preformed on it. The fact that the sample that had growth of nanofibers had growth in a low amount of time (only one minute) is similar to results that show the growth of CNTs (up to 10μm long) is also rapid under the right conditions and can occur in as little as one minutes as well [38].

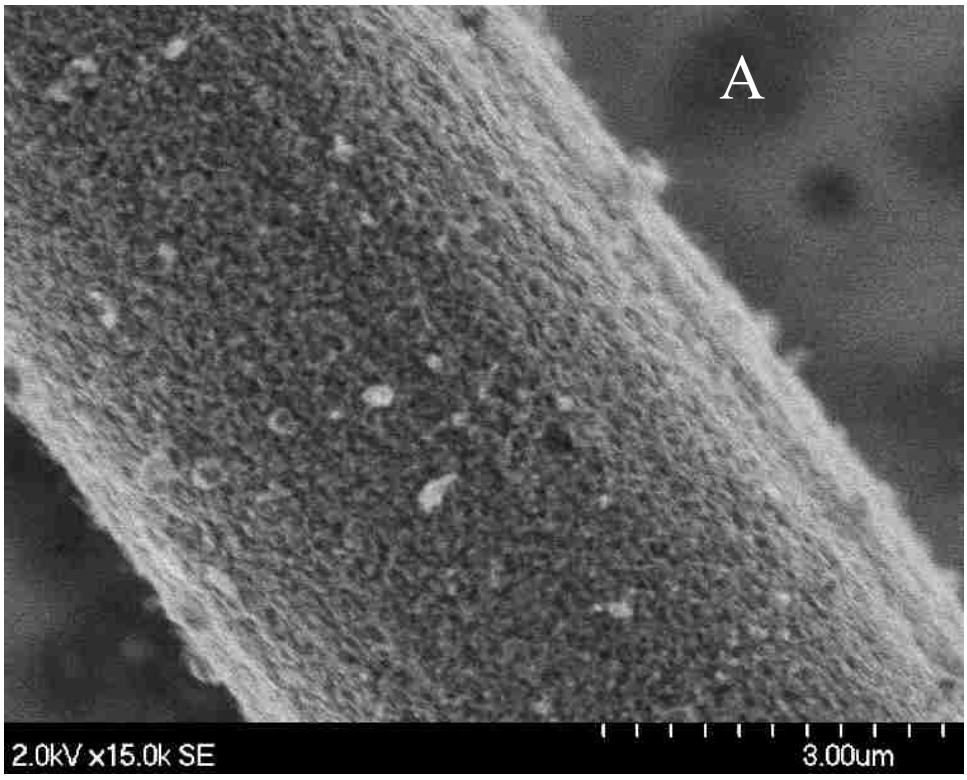

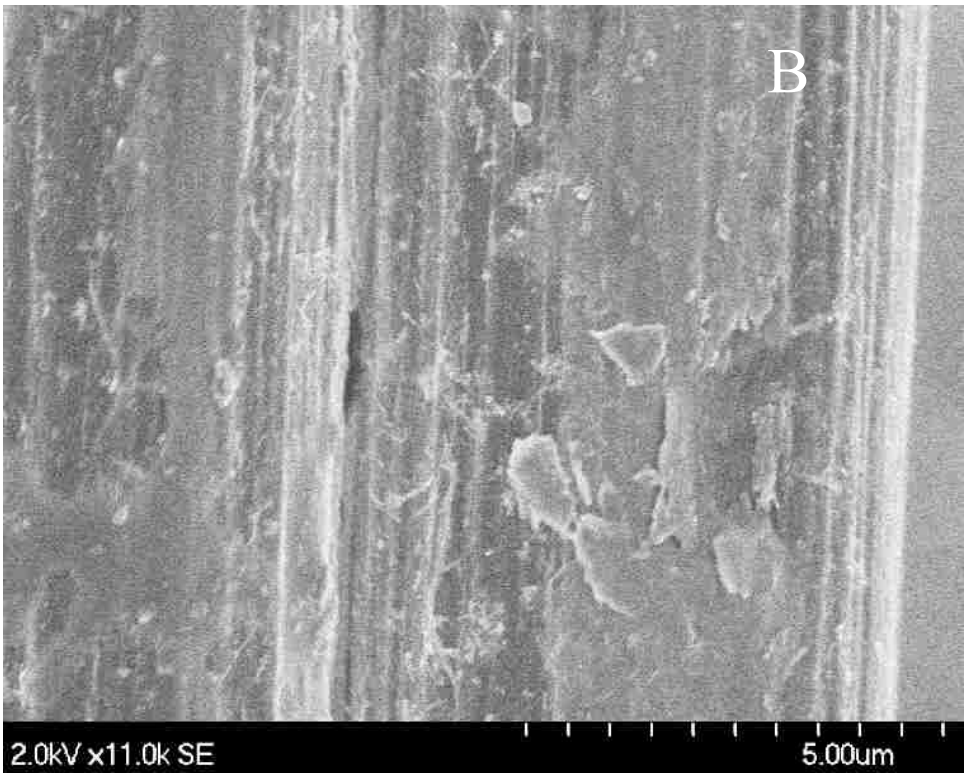

Figure 3.8-4 Samples after one minute deposition using the (a) sonicated incipient wetting protocol and the (b) non-sonication incipient wetting protocol

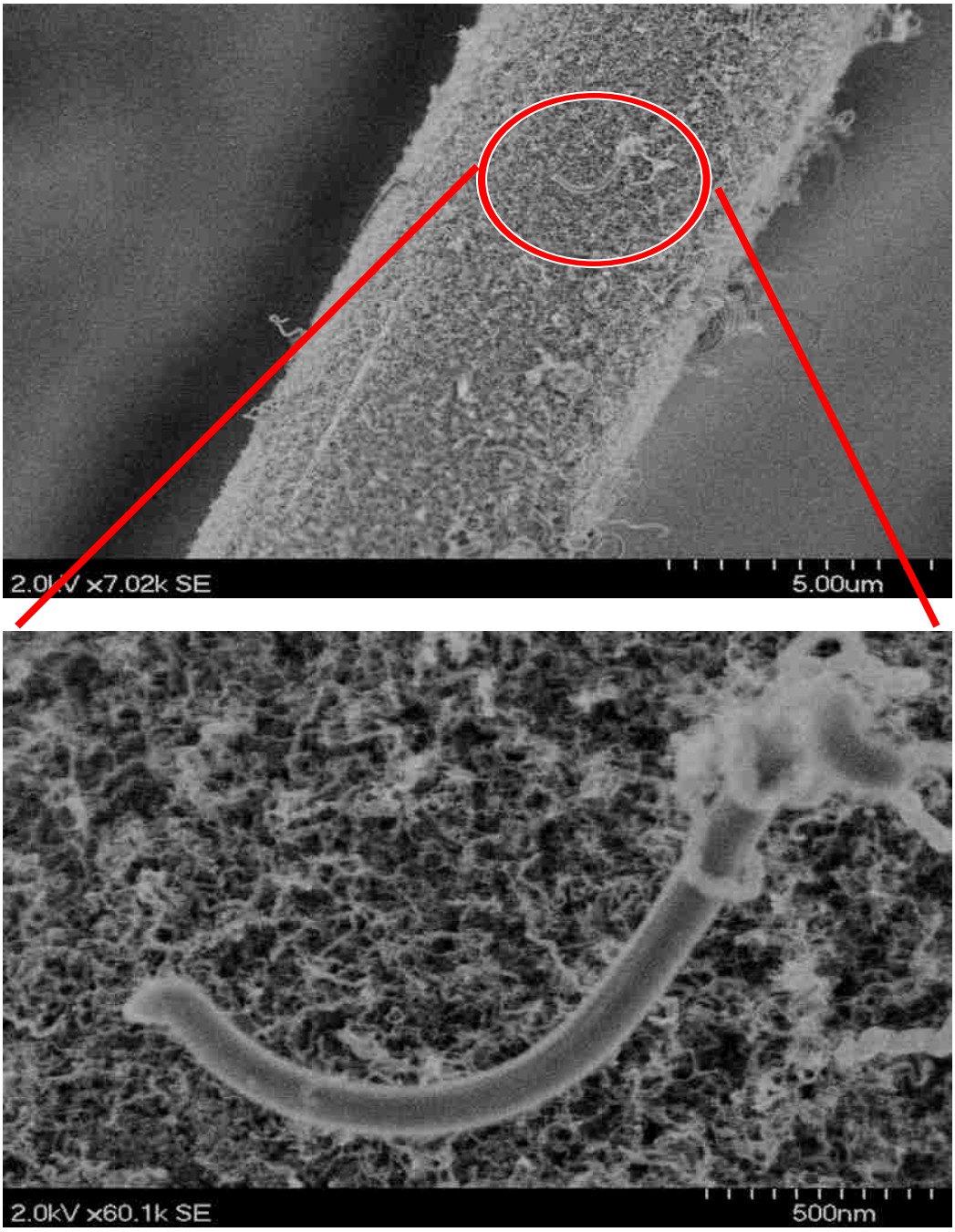

Figure 3.8-5 Sonicated sample after 5 minute deposition showing 2 modes of growth

From the SEM micrographs taken of the samples after deposition it is clear that agitating the carbon fiber via a magnetic stir rod is not sufficient. Ultrasounds sonication however, appears to be effective in spreading the catalyst across the entire carbon fiber sample. It

should be noted that 90 mg of carbon fiber is not a trivial amount of sample to try to deposit an aqueous solution on uniformly while employing a procedure that is automated (like leaving the syringe pump to deposit the catalyst in this case). After observing growth on the sonicated sample it is valuable to look at the size of the nanoparticles after incipient wetting. Simply evaporating ¼ of the solution at a time on a hotplate proved to produce various sizes of nanoparticles. Therefore the particles from the sonicated sample were expected to be far more uniform and on the nanometer level (<100 nm diameter). Interestingly, two different sizes of the Pd particles were observed with the sonication method as well. Figure 3.8-6 shows what is believed to be an agglomeration of Pd particles and 'islands' of Pd. particles. Note that a single fiber did not display both morphologies (unlike previous trials). The dark image showed in (b) shows a scanning electron image taken with the backscattering technique at a voltage of 5.0 kV in order to detect x-rays which are 'backscattered' from the sample. The light region of the debris indicates it is not a polymer and thus likely the metal deposited on the fiber due to the fact metals eject high energy electrons (used to from the 'backscattered image) from their inner shells when bombarded with the high energy incident electron beam.

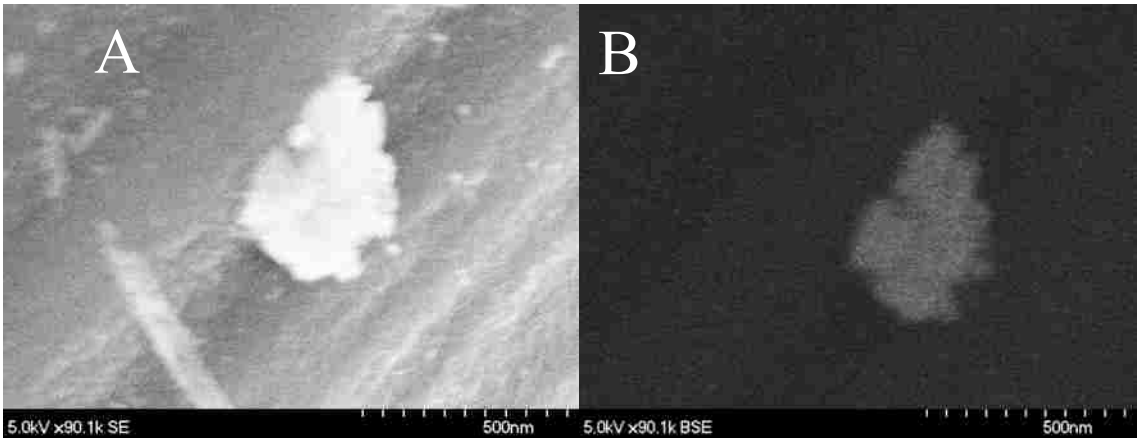

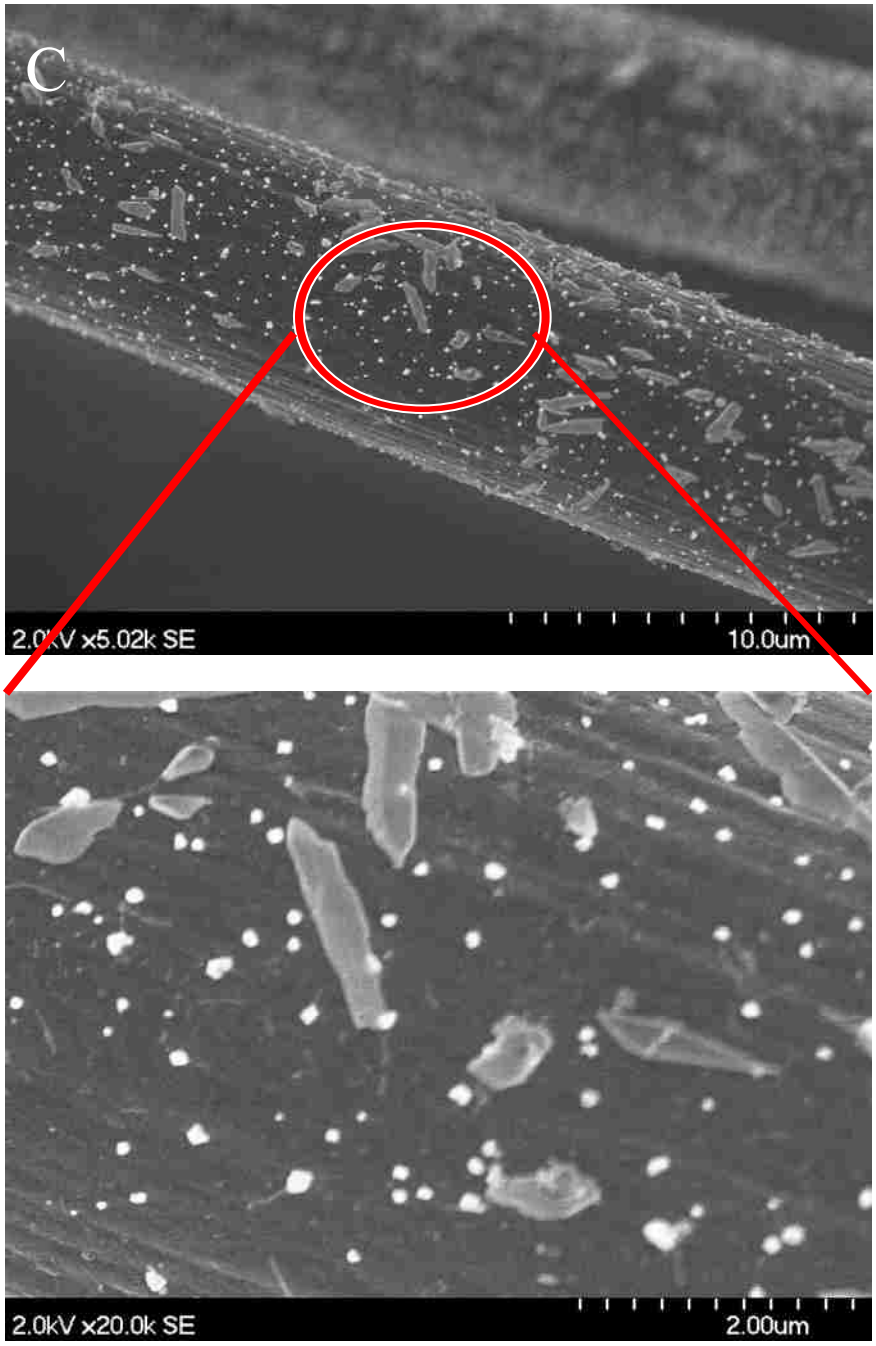

Figure 3.8-6 Sample after incipient wetting with sonication showing an agglomeration of Pd particles via (a) scanning electron micrograph and (b) backscattered electron micrograph. (c) shows islands growth of Pd particles

The islands of Pd generated on some of the carbon fiber are on the nanometer scale (c.a. 75-100 nm). The fact that some parts of the sample have agglomerations of the catalyst and some have islands demonstrates that the carbon fiber sample can not be stationary.

3.9 Effect of changing the carbon fiber substrate

The GSD protocol can be applied to pitch based fibers as well. Figure 3.9-1 shows a fiber with 35 minute deposition time. Here the low level of growth of filaments is observed especially in (b) at a high magnification. No noticeable difference between the PAN based fibers and the pitch based fibers is seen under the scanning electron microscope.

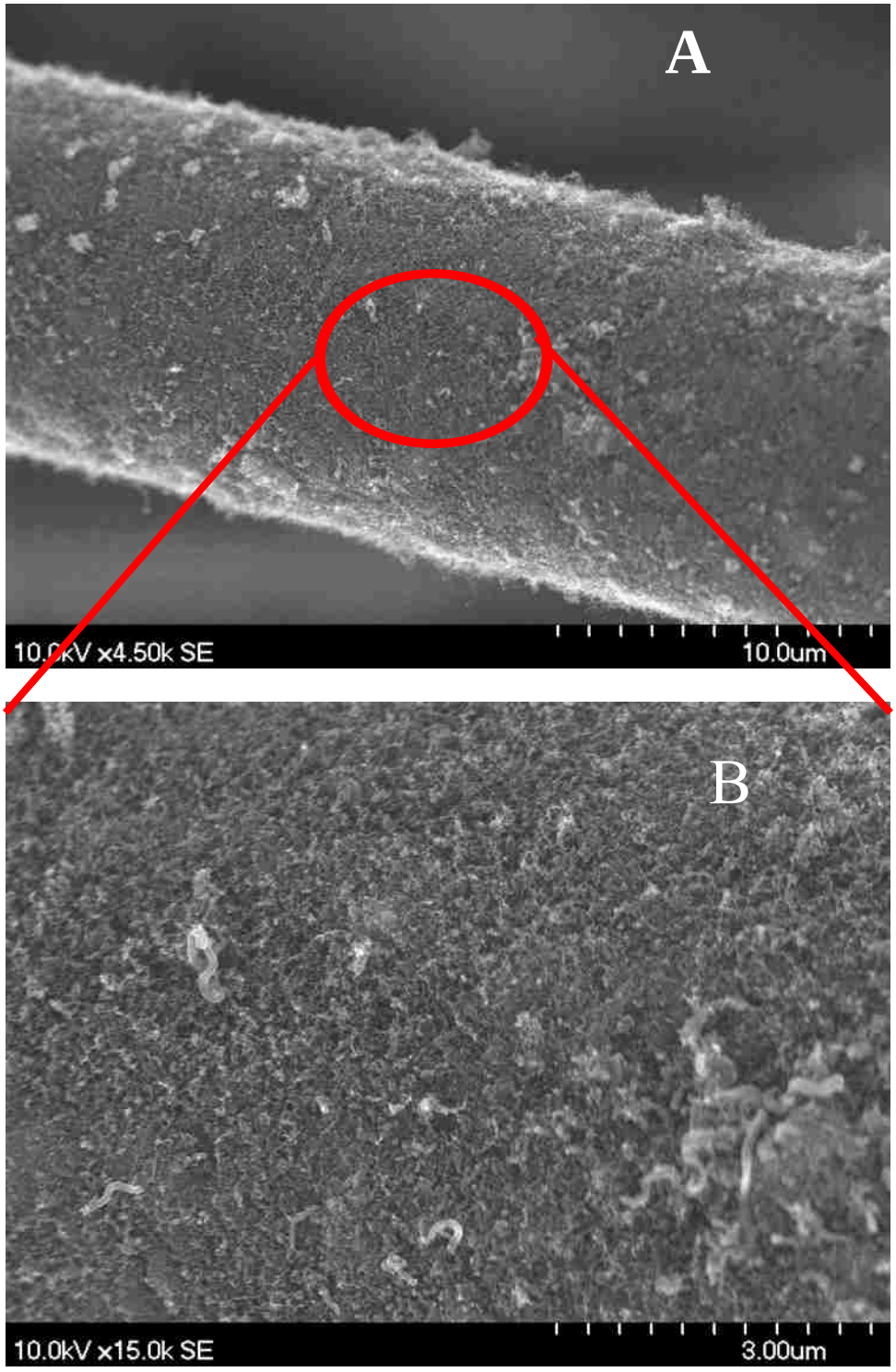

Figure 3.9-1 Pitched based fiber with deposition time of 35 minutes showing uniform coating of nm scale filaments

The process also can be applied to long PAN based carbon fibers (c.a. lengths of 12-15``). Figure 3.9-2 shows micrographs of the fibers after deposition for 35 minutes using Palladium as the metal catalyst (Palladium Nitrate (II) Hydrate as the metal salt) at an actual temperature of ~400°C using the Lindberg Blue-M furnace. The fibers were wrapped to standard XRD holders at each end to ensure the fibers would be suspended and that the combustion mixture could reach the entire surface of the fiber. Two layers of growth are once again seen as was the case on the short chopped PAN carbon fibers. Interestingly, the process was performed on the long carbon fibers with no 'activation by burning' step indicating contradicting results from using the chopped short carbon fibers as a substrate in which uniform growth was not seen without the activation step.

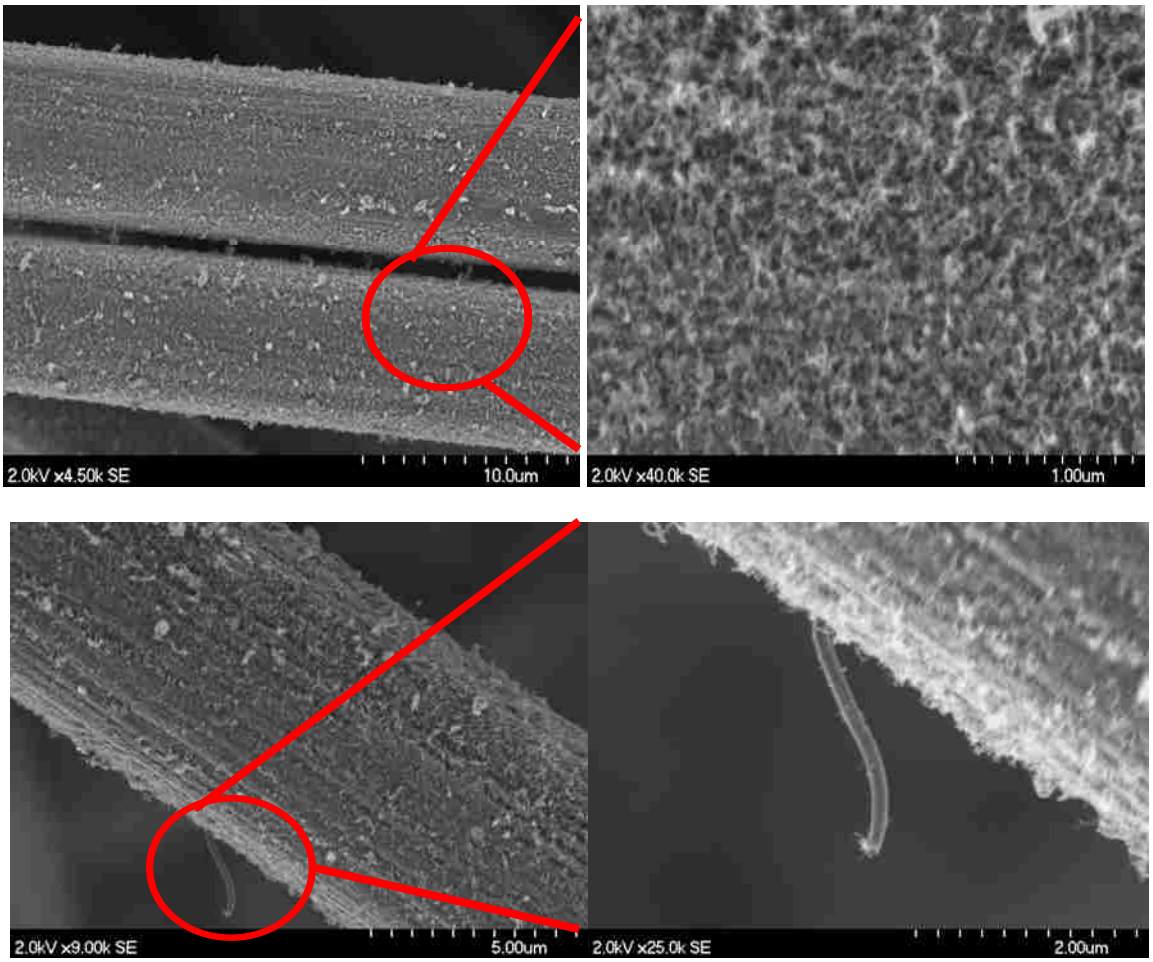

Figure 3.9-2 Micrographs of long PAN based fibers after 35 minute deposition

3.10 *Transmission Electron Microscopy (TEM) Characterization*

A transmission electron microscope is a characterization technique in which electrons are shot through a thin specimen in order to produce a micrograph. This micrograph has many potential uses including seeing nanosized particles and the even the grain structure of a sample. For preparation of carbon fiber specimens a very short carbon fiber (c.a. 3.5 mm long) was laid upon a carbon coated copper grid and then clamped down on a standard sample holder. A JEOL 2010 high resolution transmission electron microscope (HRTEM) was used for characterization.

A TEM micrograph is shown in Figure 3.10-1 to illustrate the relative diameter (~100 nm) of the larger filaments grown under the GSD process for 35 minutes. It can also be seen that the filament growth is tip based due to the metal particle being found at the tip of the filament. Also worth noting is that the filament with the metal particle appears to be hallow indicating some carbon nanotubes (either MWCNT or SWCNT) may be generated during the GSD process.

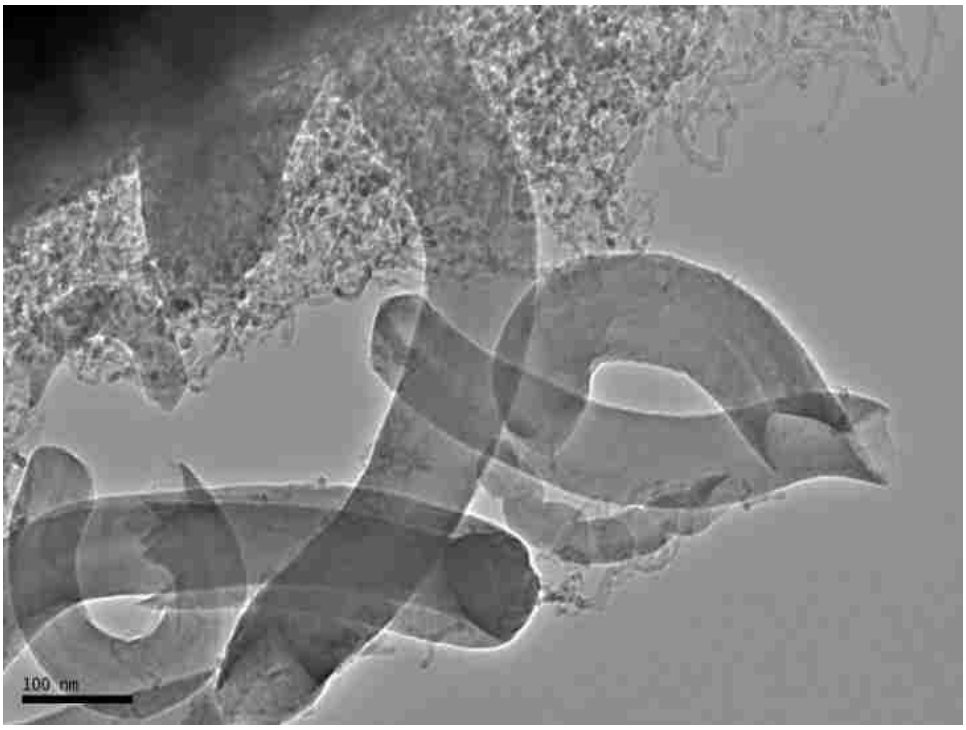

Figure 3.10-1 Transmission Electron Micrograph showing 2 layers of filament growth and proof of tip-based growth (scale of 100 nm).

Evidence that the filament growth is homogenous (90 minute deposition time) is given in the TEM micrograph shown in Figure 3.10-2. Note that even under extremely high magnification of the TEM (e.g. x 500K) a coating of filaments (~500 nm thick) around the parent carbon fiber can be seen. These filaments shown represent the carpet like

coating that could not be fully observed under SEM.

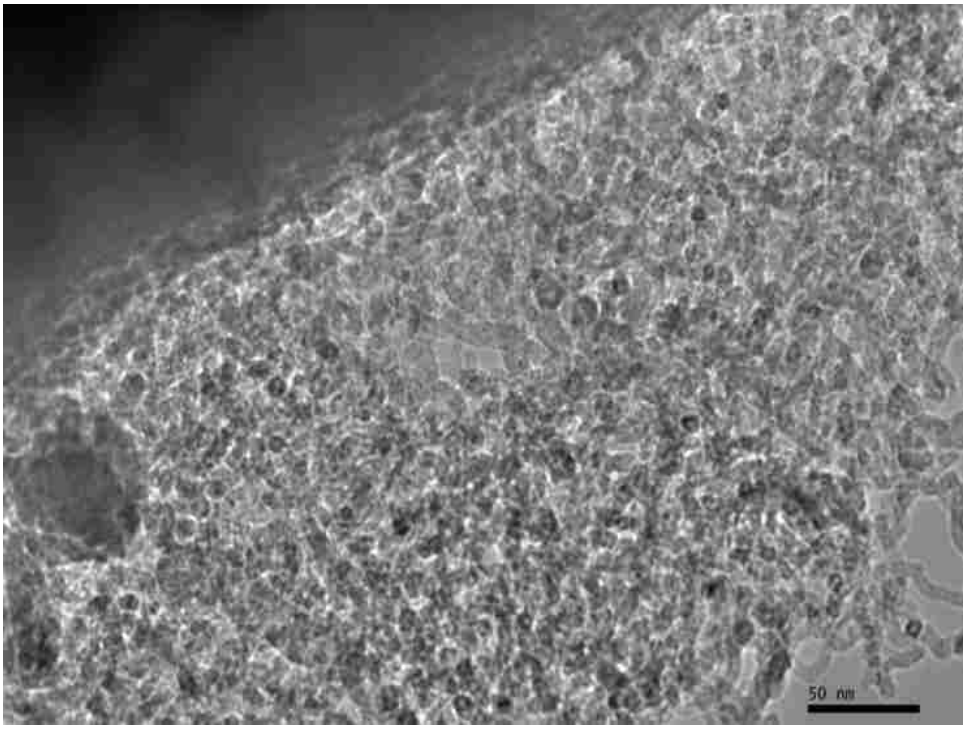

Figure 3.10-2 Transmission Electron Micrograph showing parent fiber (dark upper left corner) and nanofilaments (lighter bundle coming off of parent fiber). (scale of 50 nm)

Using PAN based carbon fibers that underwent the GSD process with the ULL protocol, the degree of crystallinity can be observed in the CNFs through the use of lattice fringes. Figure 3.10-3 shows that the crystal planes (represented as the lattice fringes) are not parallel and are at various orientations. Due to this observation it is determined that the CNFs themselves are not very crystalline (leading to an observation that the filaments generated are amorphous in character). Figure 3.10-3 also shows that the growth mechanism is tip based confirming an earlier result of the scanning electron micrographs.

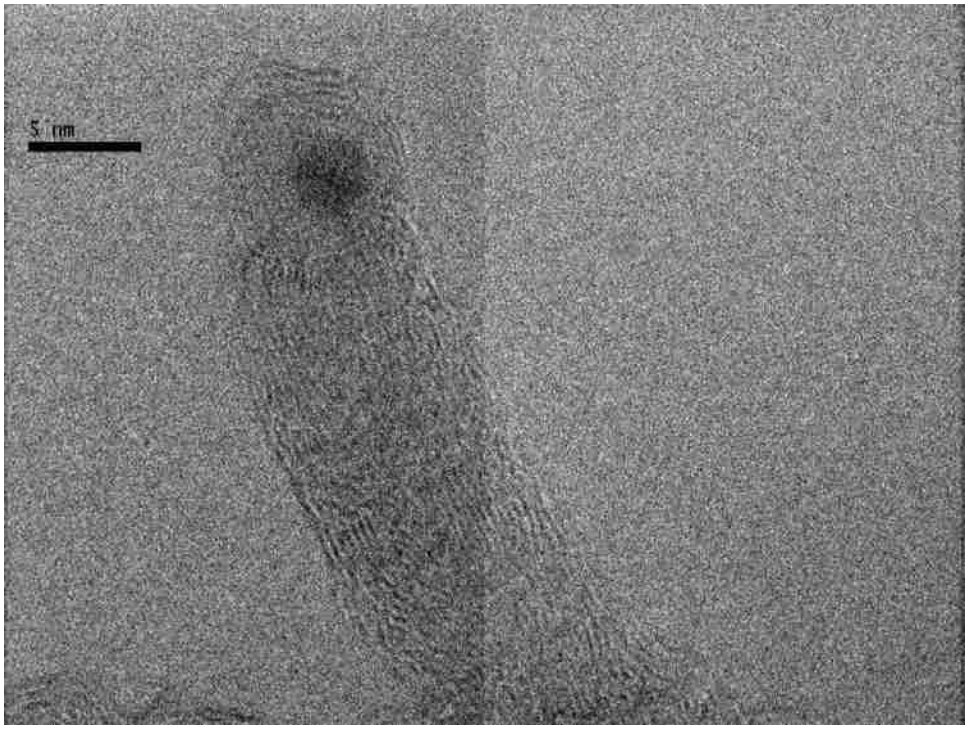

Figure 3.10-3 Transmission Electron Micrograph showing amorphous character and tip based growth.

3.11 X-Ray Diffraction Characterization

X-Ray diffraction is a non-destructive analytical technique used to characterize the crystallographic structure of a material. The scattering phenomenon of X-ray diffraction is described in Bragg's law (first formulated by W.L. Bragg) which is given by

$$n\lambda = 2d\sin(\theta) \qquad (3.1)$$

where n represents the order of diffraction, λ represents the wavelength, d represents the distance between crystal planes, and θ represents the angle of incidence. Figure 3.11-1 shows a visual schematic of Bragg's law.

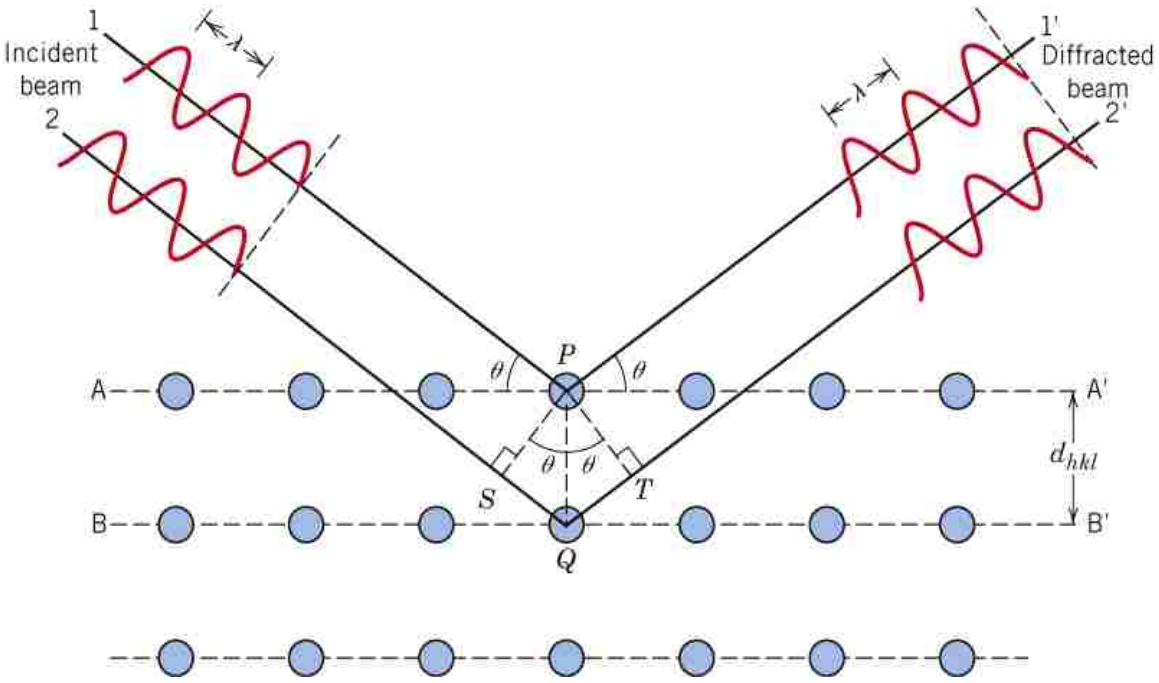

Figure 3.11-1: Schematic of X-Rays being diffracted by a crystal illustrating physical meaning of variables in Bragg's law [39]

For this analysis, an XRD diffractometer in the Department of Earth and Planetary Sciences at the University of New Mexico was used. It was equipped with a Scintag Pad V diffractometer with Data 4 software from MDI, Inc. A Bicron scintillation detector with a pyrolitic graphite curved crystal monochromator was used to apply CuKα radiation. The Jade 6.5 software was used to analyze the data by using the ICDD (International Center for Diffraction Data) database for phase identification.

Figure 3.11-2 shows the diffractogram from the PAN based short chopped fibers with CNFs resulting from 90 minute growth. This growth protocol had yielded the most uniform growth. The diffractrogram revealed only a weak and rather broad peak for all samples near 25.5° 2θ indicating an amorphous or turbostratic carbon structure based on

comparison with forms of graphite from in the database. No appreciable signal that wasn't noise was detected for the Pd itself indicating the signal was washed out by the carbon signal. Figure 3.11-3 shows the diffractogram of the bare (sizing removed) PAN based fibers demonstrating a sharp peak indicating the carbon is highly ordered and of good quality from the manufacturer.

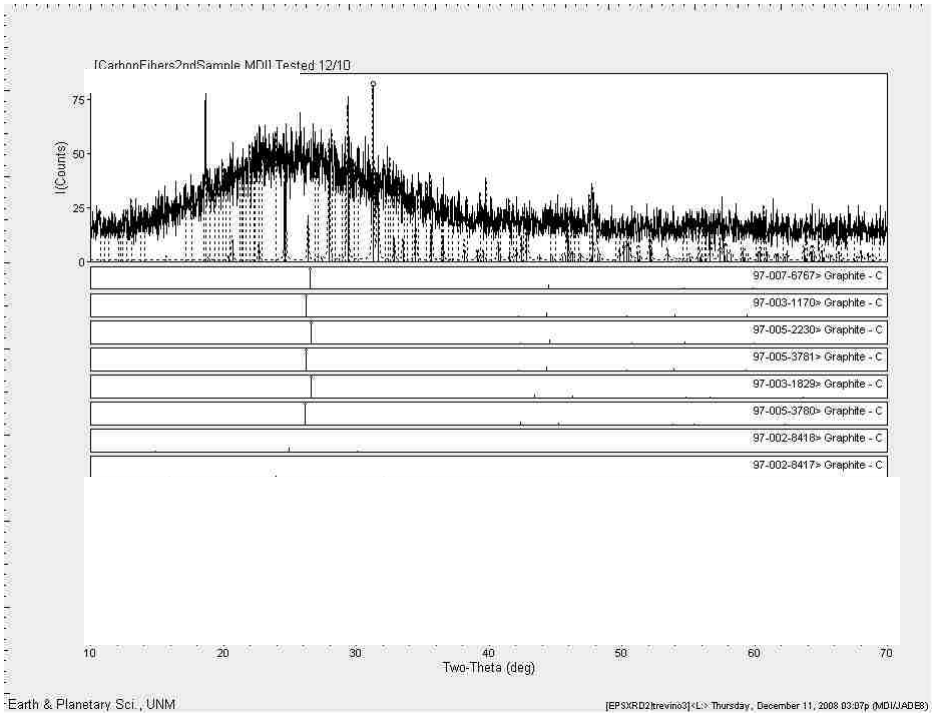

Figure 3.11-2: XRD diffractogram of Carbon Fibers with CNF from 90 minute growth protocol 0.5% loading of Pd

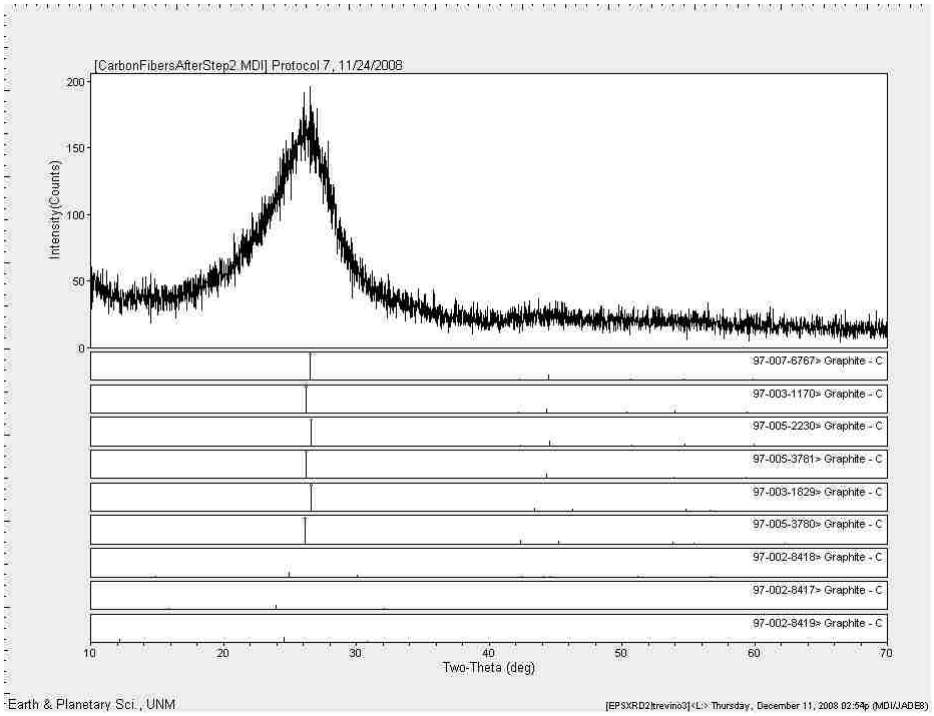

Figure 3.11-3 XRD diffractogram of bare PAN short chopped carbon fibers

3.12 *Temperature Programmed Oxidation*

Temperature programmed oxidation was used (Netzsch STA 409 PC Luxx) to compare the level of graphitization of the parent fiber with filaments. Four samples were compared: pan based 'short' carbon fibers with filament growth (90 minute deposition time) with Palladium removed via the use of aqua regia, pan based 'short' carbon fibers with the sizing removed, graphite flakes (e.g. the most graphitic form of carbon), and pryolyzed sugar (amorphous carbon). Figure 3.12-1 shows the TPO curves as weight % versus time. Following is detailed descriptions of how each was prepared:

- **Amorphous Carbon:** Carbon from pryolyzed sugar made by heating commercially purchased sucrose to 1000 C.

- **Carbon Fibers (Sizing Removed):** Commercially Purchased Pan based Carbon Fiber (Toho Tenax) were treated in a tubular furnace at 525 ^{o}C in O2 (100 sccm flow) for 10 minutes. The treated fibers were removed, rinsed in ethyl alcohol on a sieve and dried in air at 100 ^{o}C for 1 hour.

- **Carbon Fibers with Filaments (Pd. Removed):** Prepared by standard process with a growth time of 90 minutes (time the sample was exposed to the fuel mixture). The sample was placed into a vial and aqua regia (~2 cc) was added. Sample was in vial with aqua regia for 34 days. After 34 days, about ¾ of the aqua regia was removed from the vial via a dropper into a waste container. Then new aqua regia was added via a dropper. This procedure was repeated twice. Sample was allowed to sit like this for 1 day. After 1 day, all the aqua regia was removed (via a dropper again) from the vial with the sample. Then the vial with the sample in it was filled with distilled water. After this step, the water along with the fibers was poured onto a funnel to filter the water. With the sample on the funnel, it was rinsed 2 more times with distilled water. Then the sample was put into a combustion boat (covered in aluminum foil with holes punched in) and allowed to dry overnight in air underneath a fume hood.

- **Graphite:** Graphite flakes were purchased from Alfa Aesar. The flakes have a median diameter of 7-10 micron and are 99% (metals basis).

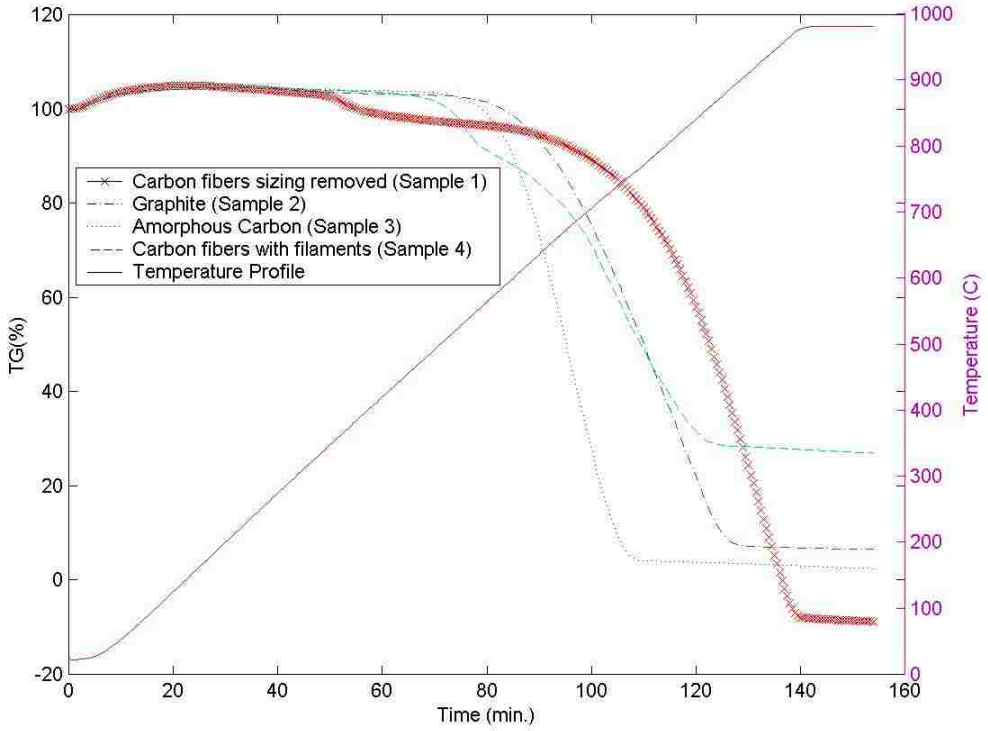

Figure 3.12-1 Comparison of different levels of graphitization of carbon including carbon fibers with filaments

From Figure 3.12-1 it can be seen that as expected the amorphous carbon lost the most weight during the treatment. Unexpectedly however the first sample to begin burning was the raw PAN based carbon fibers which are not very graphitic in nature [40]. This is especially contradictory given that a pure form of graphite (the graphite flakes) was also used. This indicates that there is an issue with the burning of both carbon fiber samples (with sizing removed and with the CNFs). Another confirmation of this result is that the carbon fiber with filament sample did not burn completely which could be due to a large number of reasons including that the fibers could have been so tightly packed as to resist the oxidation more than normal.

CHAPTER 4: CONCLUSIONS AND FUTURE WORK

4.1 Basic Observations about GSD Protocol

A new procedure has been used to synthesize carbon filaments (nanofibers) on the surface of carbon fibers thus producing multi-scale carbon fibers. This procedure serves as a relatively low temperature (c.a. 550 °C) and simple alternative to various other carbon filament/nanotubes producing methods [21, 22, 24, 25, 27, 30, 31]. Moreover its simple relatively inexpensive experimental setup utilizing an ordinary tube furnace is readably scalable.

The procedure is derived from a process called Graphitic Structures by Design (GSD) where a fuel rich combustion mixture (oxygen and ethylene) at atmospheric pressure drives growth of the carbon nanostructures (in this case carbon filaments). The procedure uses a metal catalyst (Pd) and results in rapid (>10 microns/hour) growth of the filaments. From previous studies of the GSD process [32] it assumed the carbon atoms in the filaments are formed from homogenously generated radicals (e.g. CH_2) reacting with Pd catalyst particles (e.g. CH_2 -> C + H_2). It is also presumed that the formation of the filaments is similar to the 'root mechanism' (carbon atoms transporting through or around a catalyst particle due to a chemical potential gradient) that is frequently described in literature [8, 18, 41].

An unexpected result of the process was the generation of 'three scale' carbon materials under the right conditions. That is, carbon materials with three different size characteristics were produced: i) micrometer scale commercial PAN or pitch fibers, ii) a layer of 'long' submicrometer diameter scale carbon filaments, and iii) a dense layer of 'short' nanometer diameter filaments**.** Two factors were shown to contribute to whether the Pd impregnated fibers had a bimodal distribution: (i) loading of Pd. onto the carbon fiber where loadings <0.5% tended to only produce the 'short' layer and (ii) growth time (i.e.. time when the hydrocarbon is being deposited) where growth times > 35 minutes tended to produce the two layer growth.

4.2 Effect of Parameters on Filament Size

It has been shown that certain parameters have been found to vary the size of the filaments produced. For instance, with Pd grown filaments time is the main variable to be controlled CNFs (35 minutes already being established as the 'critical' transition time between one and two layer growth of CNFs). Also 'activating' the surface of the parent fibers prior to metal catalyst impregnation decreases the size of the filaments produced when Pd is used as catalyst. It's hypothesized that activating the surface of the fiber with oxygen groups helps to anchor the metal particles to the point that they do not sinter (leading to a homogenous distribution of metal nanoparticles on the parent fiber). This point is furthered by SEM micrographs taken of the fibers directly after loading of the metal where the metal particles are no longer observable at the SEM scale. The contrast of this is the initial trials of the loading of the metal where the metal completely encased

the carbon fibers. Thus improving the engineering by lowering the metal loading needed for filament generation also aids in the controlling the size of the filaments produced.

4.3 Effect of Position in Chamber on CNF Growth

The Pd trials had shown that there is a clear dependence of CNF growth on the location of the sample in the chamber during deposition.. In general the best location for CNF generation is closer to the gas outlet downstream from the gas flow while the worst results are seen when samples are placed near the gas inlet. Similar results were seen before for carbon structure generation in a tube furnace [32]. The cause of these results can be traced back to two main parameters (i) the potency of the combustion mixture (relating to the gas flow velocity of the mixture along the length of the chamber) and (ii) the large temperature gradient along the chamber found in both the furnaces used for experiments.

4.4 Effect of substrate on CNF growth

It has been demonstrated that both PAN and pitch carbon fibers can be used as substrates for CNF growth when Pd is used as a catalyst. When run under the same conditions using Pd both pitch and PAN fibers produce very similar results as described in section 3.11. When Ni is used as a catalyst pitch fibers have produced CNFs but PAN based fibers have not. In the cases of the pitch fibers with CNFs it was observed that the fibers produced are very brittle and cleave very easily in a person's hand. The PAN based fibers however maintained their ductility even after going through the full procedure albeit without successful growth of filaments. Based on the ability to maintain its ductility PAN

fibers seem like the natural candidate to be used as a reinforcing component (with CNFs grown) in a composite for a structural reinforcement application.

4.5 Effect of Temperature on CNF growth

It has been demonstrated that with the GSD protocol CNFs can be grown using Palladium as a catalyst at a temperature as low as 550°C. This makes the GSD process one of a few protocols that can generate a uniform coating of CNFs on a substrate at a temperature <600°C. It should be noted that the CNFs were grown in an ethylene-oxygen environment opposed to a ethylene-hydrogen environment like the one used by Downs and Baker to generate CNFs at 600°C[42]. Also the GSD process does not use a vacuum chamber which is necessary if one is to obtain CNFs at a very low temperature range of 200-400°C (using dc PECVD vacuum chamber and cobalt colloid) [43].

4.6 Effect of 'Enhanced Parameters' on CNF growth

A few parameters have been varied on the CNF growth protocols in order to increase the likelihood for growth: (i) fuel rich mixture (i.e.… higher gas flow of ethylene), (ii) longer growth times and (iii) increase metal loading (1% loading of the catalyst vs. the standard 0.5%). The second parameter has been shown to increase in longer filaments as intuitively expected. It was shown running the deposition of the hydrocarbon for longer than 35 minutes results in a secondary layer of CNFs generated. The longest growth time ran was 270 minutes which was run for the ultra low loading (0.5%) protocol using Palladium. In this case running for longer time allowed for CNFs to be grown that were large enough (sub-micron level diameters) to be observable under SEM. Using the ULL

at 35 minutes did not result in any SEM observable CNFs. Therefore because the metal loading was decreased it, the growth time had to be increased to generate CNFs of the same size as those made with the standard loading.

4.7 Future Work of CNF Growth Protocol

- For the purpose of scaling up the process for industrial use, the incipient wetting protocol will have to be modified. The current protocol has some legitimate issues: (i) homogenous distribution of the IWS can not be guaranteed as the process is manual and prone to much human error and (ii) the evaporation step involves the sample being in a combustion boat which meaning that the entire sample is not exposed to air at the same time. It is reasonable to speculate that both of these issues could be why often times CNF growth is not homogenous throughout the entire fiber (seen throughout the course of the research despite numerous changes in the incipient wetting protocol). Sputtering seems a better candidate to replace the incipient wetness procedure as it would assure a far more homogenous distribution of the catalyst and is also a standard of both industry and research involving CNF synthesis.
- A good study of the process of CNF generation would involve determining the absolute minimum conditions needed for CNF growth to occur. These conditions include the minimum growth time needed, the minimum fuel mixture (in terms of flow rate and number of gases) and the minimum amount of metal loading of the catalyst needed. Knowing these conditions would help one to craft a true optimization of the protocol where the least amount of material and energy would

be used to generate CNFs. Both the role of the growth time and metal loading have already been investigated to some degree: (i) it was shown that a metal loading of 0.5% could still be used to generated CNFs under the correct conditions and (ii) CNFs could be grown in as little as one minute under the correct conditions. However the future work proposed would require numerous trials to generate enough data to be statistically relevant for one to conclude what the optimized repeatable protocol is for this process.

- For the sake of robustness and optimization of the process, other metals should be explored as catalysts for the process. Likely candidates include Fe , Co, and Ni as these transition metals have been used often to generate CNFs. Also alloys should be considered such as Cu/Ni in order to determine if having an alloy instead of a sole catalyst increases the distribution and yield of CNFs generated with the process. Further information could also be learned about the chemical nature of different metal catalysts during growth such as if burning of the carbon fiber prior to catalyst impregnation increases the nucleation sites on the fiber (leading to better CNF distribution) for all the chosen metals/alloys or only some.

4.8 Future Application of Research

The research conducted in this thesis was conducted with the goal to investigate the feasibility of growing CNFs on the surface of carbon fibers toward producing hybrid reinforcements for novel polymeric composites. This goal has been fulfilled in the scope of the work presented. However future work would be to test a composite of the multiscale carbon fibers for improved properties of the composite.

The surface-grown CNFs could be thought of as mechanical interlocks between the microscale carbon fibers and the polymeric matrix. In this application, the role of the carbon nanotubes would be analogous to the bumps found on rebar used in reinforced concrete which serve to better adhere the rebar to the concrete. Increased adhesion between the carbon fibers and the matrix (whether it be concrete, epoxy or other) would result in a better transfer of shear strength to the carbon fibers; thus utilizing the fiber's high axial strength and helping to prevent dislodgment of the fibers from the matrix, a common form of composite failure, which is shown in Figure 4.8-1.

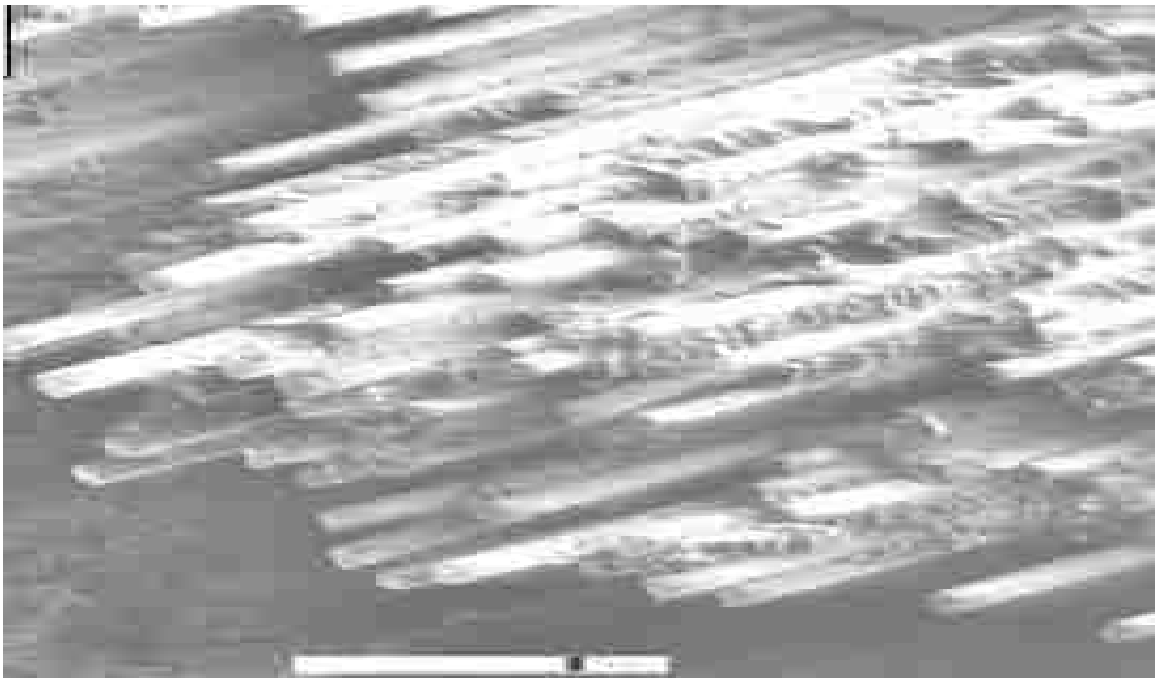

Figure 4.8-1 Fiber Pullout: fracture surface from tensile test [44]

Other groups that used CVD to synthesize CNFs have already tested multiscaled carbon fibers in a composite [29, 30] where they found that having CNFs on the carbon fiber led to an improvement of mechanical properties (15% in interfacial strength and 20% in

flexural strength compared to composites using bare fibers). Testing the performance of composites with multi scale fibers from the current work would demonstrate if improved composites could be made with multi-scale fibers generated from a much simpler, cheaper process. Various test instruments could be used to determine the triboilogical and mechanical properties of the multi-scale fiber composite such as a nanoindenter (adhesion tests) and a micro tensile machine (adhesion of fiber and matrix).

REFERENCES

1. Iijima, S. *Helical microtubles of graphitic carbon.* Nature, 1991, **354**: 56-58.
2. Kim, H. *Iron particles in carbon nanotubes* Carbon, 2005, **43**: 1743-1748.
3. Aubuchon, J.F., C. Daraio, L. Chen, A.I. Gapin, and S. Jin. *Iron Silicide Root Formation in Carbon Nanotubes Grown by Microwave PECVD.* The Journal of Physical Chemistry, 2005, **109**: 24215-24219
4. Edwards, B.C. *Design and development of a space elevator.* 2007, **47**: 735.
5. Radushkevich, L.V. and V.M. Lukyanovich. *About the structure of carbon formed by thermal decomposition of carbon monoxide on iron substrate.* Zurn Fisic Chim, 1952, **26**: 88-95.
6. Hughes, T.V. and C.R. Chambers, *Manufacture of Carbon Filaments*, U.S. Patent, Editor. 1889: .
7. Frank, I.W., D.M. Tanenbaum, A.M.v.d. Zande, and P.L. McEuen. *Mechanical properties of suspended graphene sheets.* Journal of Vacuum Science & Technology: Part B, 2007, **25**(6): 2558-2561.
8. Melechko, A.V., V.I. Merkulov, T.E. McKnight, M.A. Guillorn, K.L. Klein, D.H. Lowndes, and M.L. Simpson. *Vertically aligned carbon nanofibers and related structures: Controlled synthesis and directed assembly.* Journal of Applied Physics 2005, **97**: 041301-041338.
9. Yun Zhao, Chunhua Li, Kelu Yao, and J. Liang. *Preperation of carbon nanofibers over carbon nanotube-nickel catalyst in propylene decomposition.* Journal of Material Science 2007, **42**: 4240-4244.
10. Jong, K. and J. Geus. *Carbon Nanofibers:Catalytic Synthesis and Applications.* Scientific Engineering, 2000, **42**(4): 481-510.
11. Dai, H., A. Rinzler, P. Nikolaev, A. Thess, D. Colbert, and R. Smalley. *Single-wall nanotubes produced by metal-catalyzed disproportionation of carbon monoxide* Chemical Physical Lettters, 1996, **260**: 471-475.
12. Deng, W., X. Xu, and W.G. III. *A Two-Stage Mechanism of Bimetallic Catalyzed Growth of Single Walled Carbon Nanotubes* Nano letters, 2004, **4**(12): 2331-2335.
13. Jong, W.J., S.H. Lai, K.H. Hong, H.N. Lin, and H.C. Shih. *The effect of cataysis on the formation of one-dimensional carbon structured materials.* Diamond and Related Materials, 2002, **11**: 1019-1025.
14. Krishnankutty, N., N.M. Rodriguez, and R.T.K. Baker. *Effect of Copper on the Decomposition of Ethylene over an Iron Catalsy.* Journal of Catalysis, 1996, **158**: 217-227.
15. Tao, X., X. Zhang, J. Cheng, Y. Wang, F. Liu, and Z. Luo. *Synthesis of novel multi-branched carbon nanotubes with alkalil-element modified Cu/MgO catalyst* Chemical Physical Letters, 2005, **409**: 89-92.
16. Park, C. and M.A. Keane. *Growth of Filamentous Carbon from the Surface of Ni/SiO2 Doped with Alkali Metal Bromides.* Journal of Colloid and Interface Science, 2002, **250**: 37-48.
17. Volmer, M. and A. Weber. *Nuclei formation in supersaturated states. Z.* Phys. Chem., 1925, **119**: 277.

18. Dupoise, A. *The catalyst in the CCVD of carbon nanotubes-a review.* Progress in Materials Science, 2005, **50**: 929-961.
19. Rodriguez, N.M. *A review of catalytically grown nanofibers.* Journal of Materials Research, 1993, **8**: 3233-3248.
20. Goodman, D.W. and J.E. Houston. *Catalysis: New Persepectives from Surface Science.* Science, 1987, **236**: 403-409.
21. Terrones, M., A.M. Benito, C. Manteca-Diego, W.K. Hsu, O.I. Osman, J.P. Hare, D.G. Reid, H. Terrones, A.K. Cheetam, K. Prassides, H.W. Kroto, and D.R.M. Walton. *Pyrolytically grown BxCyNz nanomaterials: nanofibres and nanotubes.* Chemical Physical Lettters, 1996, **257**: 576-582.
22. Endo, M., K. Takeuchi, K. Kobari, K. Takahashi, H. Kroto, and A. Sarkar. *Pyrolytic Carbon Nanotubes from Vapor-Grown Carbon Fibers* Carbon, 1994, **33**(7): 873-881.
23. Baker R.T.K., D.W.B. *Novel Fiber-Carbon Filament Structures.* Carbon, 1991, **29**: 1173-1179.
24. Zhu, S., C.-H. Su, S.L. Lehoczky, I. Muntele, and D.Ila. *Carbon nanotube growth on carbon fibers.* Diamond and Related Materials, 2003, **12**: 1825-1828.
25. Sonoyama, N., M. Ohshita, A. Nijubu, H. Nishikawa, H. Yanase, J.-i. Hayashi, and T. Chiba. *Synthesis of carbon nanotubes on carbon fibers by means of two-step thermochemical vapor deposition.* Carbon, 2005, **44**: 1754-1761.
26. Organization, I.L. *International Chemical Safety Card 0085*. 2002 [cited March 20th 2009]; Chemical Safety Information for m-Xylene]. Available from: http://www.ilo.org/public/english/protection/safework/cis/products/icsc/dtasht/_icsc00/icsc0085.htm.
27. Smiljanic, O., T. Dellero, A. Serventi, G.Lebrun, B.L. Stansfield, J.P. Dodelet, M. Trundeau, and S. Desilets. *Growth of carbon nanotubes on Ohmically heated carbon paper.* Chemical Physical Letters, 2001(342): 503-509.
28. site, P.S.w. *Safety MSDS data for hydroflouric acid* 2005.
29. Thostenson, E.T., W.Z. Li, D.Z. Whang, Z.F. Ren, and T.W. Chou. *Carbon Nanotube/carbon fiber hybrid multiscale composites.* Journal of Applied Physics, 2002, **91**(9): 6034-6037.
30. Mathur, R.B., S. Chatterjee, and B.P. Singh. *Growth of carbon nanotubes on carbon fibre substrates to produce hybrid/phenolic composites with improved mechanical properties.* Composites Science and Technology, 2008, **68**: 1608-1615.
31. W.Z. Li, D.Z. Wang, S.X. Yang, J.G. Wen, and Z.F. Ren. *Controlled Growth of carbon nanotubes on graphite foil by chemical vapor deposition.* Chemical Physics Letters, 2001, **335**: 141-149.
32. Phillips, J., T. Shiina, M. Nemer, and K. Lester. *Graphitic Structures by Design.* Langmuir 2006, **22**: 9694-9703.
33. Atwater, M., J. Phillips, S. Doorn, C. Luhrs, Y. Fernandez, J. Menendez, and Z. Leseman, *The Production of Carbon Nanofibers and Thin Films on Palladium Catalysts from Ethylene-Oxygen Mixtures*. 2009.
34. Hyer, M.W., *Stress Analysis of Fiber-Reinforced Composite Materials*, ed. T. Casson. 1998: The McGraw-Hill Companies, Inc. 10-14.

35. Reinhart, T.J., *Composites*. 3rd ed. Engineered Materials Handbook, ed. C.A. Dostal. Vol. 1. 1987, Metals Park: ASM International.
36. Anton, R. *Heteregenous nucleation and growth*. 2001 [cited 2009 March 10, 2009]; Available from: http://www.physnet.uni-hamburg.de/iap/group_ds/index.html.
37. Wal, R.L.V., T. Ticich, and V.E. Curtis. *Substrate-support interactions in metal-catalyzed carbon nanofiber growth.* Carbon, 2001, **39**: 2277-2289.
38. Klinke, C., *Analysis of Catlytic Growth of Carbon Nanotubes*. 2003, University of Karlsruhe: Karlsruhe. p. 94.
39. W. D. Callister, J. and D.G. Rethwisch, *Fundamentals of Materials Science and Engineering: An Integrated Approach*. 3rd ed. 2008: John Wiley and sons, Inc, .
40. Lee, S., *Handbook of Composite Reinforcements*. illustrated ed. 1992: John Wiley and Sons. 715.
41. Chen, C.K., W.L. Perry, X. Huifag, Y.B. Jiang, and J. Phillips. *Plasma torch production of macroscopic carbon nanotube structures.* Carbon, 2003, **41**: 2555-2560.
42. Downs, W.B. and R.T.K. Baker. *Novel Carbon Fiber-Carbon Filament Structures.* Carbon, 1991, **8**: 1173-1179.
43. Boskovic, B.O., V.B. Golovko, M. Cantoro, B. Kleinsorge, A.T.H. Chuang, C. Ducati, S. Hofmann, J. Robertson, and B.F.G. Johnson. *Low temperature synthesis of carbon nanofibres on carbon fibre matrices.* Carbon, 2005, **43**: 2643-2648.
44. Al-Haik, M.S., M.Y. Hussaini, and H. Garmestani. *Prediction of nonlinear viscoelastic behavior of Polymeric Composites using an artificial neural network.* International Journal of Plasticity, 2006, **22**: 1367-1392.